

A1.3 AIMS OF ANALYSIS

A1 3 1 Detailed petrographic analysis was conducted on the 12 ceramic sherds in order to characterise their raw materials and interpret their origin or 'provenance'. Aspects of the production technology of the pottery were also noted. A comparison was made between the composition of the sherds in thin section and their macroscopic classification in order to examine the correspondence between these two approaches.

A1.4 METHODOLOGY

A1 4 1 Sub-samples of all 12 artefacts were impregnated with epoxy resin and prepared as standard petrographic thin sections at the University of Sheffield, Department of Archaeology. These were studied at magnifications of x25-400 under the polarizing light microscope. The 12 sherds were classified based upon their petrographic composition in thin section. Each group of sherds was then characterised in detail under the microscope and interpreted fully in terms of its constituent raw materials and pottery technology. The thin-section petrographic analysis was compared to the macroscopic fabric classification of the same sherds. Identification of the likely source(s) of raw materials used for this 'native'-type pottery was made by comparison with geological maps and reports of the study area, as well as previous analyses of contemporary pottery from nearby sites.

A1.5 RESULTS AND INTERPRETATION

A1 5 1 **Petrographic classification and description:** the 12 sherds could be divided into three groups based upon their petrographic composition in thin section. These include a large group, with several smaller sub-groups, and a single unique sample (Table 32). Detailed descriptions of the composition and probable technology of these groupings have been compiled. Photomicrographs of each sample have been taken, as well as plates of specific features (Pls 36-8).

Petrographic Classification		Macroscopic Fabric
A66/2	Basalt-tempered	Fabric 1
A66/1	Very fine clay	Fabric 4
A66/3		Fabric 2
A66/4	Angular voids	Fabric 4
A66/6	Grog temper	Fabric 4
A66/5	Sandy clay	Fabric 1
A66/8		Fabric 4
A66/10	Sandstone inclusions	Fabric 1
A66/7	Sandy clay	Fabric 2
A66/9		Fabric 1
A66/11	Quartz, poly-quartz	Fabric 1
A66/12	Sandstone, feldspar	Fabric 3

Table 32 Thin-section petrographic and macroscopic classification of 12 late Iron Age ceramic sherds

A1 5 2 **Sample A66/2** sample A66/2 is unique among the 12 sherds analysed, in that it is characterised in thin section by the presence of poorly-sorted inclusions.

of basalt, fine rounded quartz and distinctive rounded opaque bodies in a non-calcareous clay matrix. The basalt inclusions are generally equigranular and composed of elongate plagioclase feldspar, equant clinopyroxene and opaques. They are sub-rounded to sub-angular, have a range of sizes (maximum = 2mm) and are well preserved. It is not likely that they were naturally occurring in the clay source used to produce this artefact and were probably added as temper. The angular, fresh nature of the inclusions suggests that they may derive from the crushing of pieces of basalt (Pl 36, C and D). The other inclusions in the sample are likely to have been naturally occurring. They consist of equant and elongate, sub-rounded to rounded, monoclinic quartz with undulose extinction. These vary in size (maximum = 0.96mm) but have a modal size of fine sand grade. They may have derived from the breakdown of a quartz-rich sedimentary rock, as suggested by the presence of a few rare siltstone inclusions in the sample. Fine mica occurs sparsely in the clay used to produce this sample. The rounded, equant and elongate, opaque, ferruginous inclusions that are another characteristic feature of this sample in thin section are also likely to have been naturally occurring in the clay. The vessel from which the sherd originated was fired to a temperature greater than 850°C in a weakly oxidising atmosphere. No evidence exists in thin section for the methods used to form this vessel.

A1 5 3 *Samples A66/1, A66/3, A66/4, A66/5, A66/6, A66/8, A66/10* in thin section, these seven sherds all contain conspicuous meso- and macro-voids that appear to have been produced by the degradation of inclusions (Pl 36, A). The majority of the samples also contain grog temper (Pl 36, E). The distinctive voids, which are evident in hand specimen and give the sherds a 'spongy' appearance, can have straight edges and an elongate or rhombohedral shape in thin section. They are likely to have been left by the degradation of a single type of inclusion type after firing, perhaps by solution in the archaeological record. For the most part, nothing remains of the original inclusions themselves. However, a few residual pieces in samples A66/1 (Pl 36, B) and A66/3 suggest that they were composed of the cryptocrystalline growth of a colourless, low relief, low birefringence mineral. It is not possible to identify this mineral with certainty, but it has the general appearance of chert. Chert is not known to be dissolved from pottery and is generally stable after firing. In the macroscopic analysis of sherds from SCA8, SCA15 and other sites, Vyner reports (*Section 5.1.4*) these conspicuous voids in Fabric 4 and interprets them as forming from the leaching of calcareous inclusions, perhaps gypsum. The remnants of the inclusions in samples A66/1 (Pl 36, B) and A66/3 are not dissimilar to fine-grained gypsum. Some of the remnants of these inclusions seem to have some organic matter associated with them. The angular nature of the voids, and their range of sizes, suggests that the now degraded inclusions may have come from the crushing of larger pieces of the material, which was then added as temper.

A1 5 4 Despite these shared characteristics, the seven samples can be sub-divided into three groups based upon the nature of the base clay to which the now degraded temper was added. Samples A66/1 and A66/3 appear to have had a

fine non-calcareous base clay with few inclusions, except rare quartz. Both contain grog temper from ceramics that were compositionally similar to the host and therefore appear rather inconspicuous in thin section. Samples A66/1 and A66/3 contain meso- and macro-elongate voids that are aligned to the margins of the sections. Both samples were fired at less than 850°C and have oxidised margins and a reduced core that indicates that the clay was rich in carbon and insufficiently oxidised during firing. Sample A66/3 contains some spherical organic structures within voids that could be plant remains. These do not seem to represent temper.

A1 5 5 Samples A66/4 and A66/6 are rather similar to A66/1 and A66/3 in thin section, but contain a greater abundance of mineral inclusions in their base clays. These inclusions consist mainly of moderately well-sorted sub-angular to rounded, fine sand-sized quartz inclusions. Distinctive equant and elongate, fine sand-sized, amorphous, orange-red inclusions also occur, which appear to be a breakdown product such as chlorite. A remnant of the base clay used to produce these two samples can be seen in A66/4 (Pl 37, A). Samples A66/4 and A66/6 contain less grog temper than A66/1 and A66/3. Both were fired at less than 850°C and were incompletely oxidised.

A1 5 6 The non-calcareous base clay of samples A66/5, A66/8 and A66/10 is even more inclusion-rich than the other two groups. It contains abundant moderately well-sorted sub-angular to sub-rounded fine and medium sand-sized quartz, polycrystalline quartz and white mica. This sandy clay contains occasional remains of a quartz-rich arenitic rock, which may be the source of much of the mineral inclusions. Like the other two groups, grog temper and the now degraded material were added to a base clay. Less of the latter material was added in the case of these three samples. Sample A66/5 may contain a grog inclusion with the distinctive voids within it (Pl 37, B), suggesting that ceramics with the same fabric were crushed and used as temper. All three samples were reduction-fired, with the exception of the very margin of the vessel in samples A66/5 and A66/10.

A1 5 7 *Samples A66/7, A66/9, A66/11 and A66/12* these four sherds are characterized in thin section by a sandy, non-calcareous fabric that is rich in quartz. It contains generally poorly sorted inclusions, ranging from abundant sub-angular to sub-rounded fine sand-sized quartz, white mica and feldspar, to less common sub-rounded, coarse sand-sized quartz, polycrystalline quartz and microcline. These inclusions appear to have derived from a quartz-rich sandstone, fragments of which occur in samples A66/11 and A66/12 (Pl 38). No temper appears to have been added to this sandy clay. Possible charred organic remains occur in sample A66/12. Meso- and macro-elongate voids occur in samples A66/7, A66/9 (Pl 37, E) and A66/11, which are oriented parallel to the margins of the sections. All four samples were reduced or incompletely oxidised and probably fired at less than 850°C.

A1 5 8 *Correspondence between macroscopic and petrographic classification:* whilst there is some agreement between the macroscopic fabric classification of the 12 sherds and the petrographic analysis, the two do not correspond directly to one another (Table 32). For instance, sample A66/2 was classified

macroscopically as Fabric 1, which is defined as containing 'sedimentary quartz chunks' (*Section 5.1.14*). Whilst quartz of sedimentary origin occurs in this sample in thin section, its distinguishing feature is the presence of basalt temper. The other sherds classified macroscopically as Fabric 1 (A66/5, A66/9, A66/10, A66/11) do not contain basalt in thin section. These were placed in several different petrographic groups based upon their analysis in thin section, as two contained distinctive voids from the post-firing decomposition of temper, but the other two did not. Similarly, the two samples classified macroscopically as Fabric 2 were not found to be composed of the same fabric in thin section. Only one sherd of Fabric 3 was analysed in this study. In thin section, this was related to several samples classified macroscopically as Fabrics 1 and 2. The four macroscopic Fabric 4 samples analysed in this study are related to one another petrographically, although in thin section it was possible to identify additional compositional variation between these in terms of the base clay to which the decomposed temper was added. The petrographic analysis of the 12 sherds indicates that several additional samples should have been assigned to this macroscopic fabric, as they also contained the distinctive voids left by the breakdown of angular temper.

- A1.5.9 Sherds A66/5 and A66/10, which came from different contexts, but are thought to be from the same vessel (*Section 5.1.19*), were found to have a very similar petrographic composition in thin section. Sample A66/8 was classified macroscopically as Fabric 2 (*Section 5.1.15*), but was labelled as Fabric 4 on the sample bag. Its composition in thin section suggests that it once contained the angular temper and is therefore in keeping with the definition of macroscopic Fabric 4.
- A1.5.10 It is interesting that the macroscopic analysis of the pottery did not detect the presence of grog temper, which occurs in several of the 12 samples analysed in thin section. Despite this and other irregularities, the hand specimen analysis of the ceramics captured the quartz-rich sandy nature of most of the sherds.
- A1.5.11 ***Provenance of the ceramics:*** in the macroscopic analysis of the Late Iron Age-early Romano-British material from SCA8, SCA15 and other sites in the project, Vyner describes it as 'gritty 'native'-type pottery' that is similar to other assemblages of pre-Roman Iron Age date from the area (*Section 5.1.8*). Further detailed comments on the distribution of the individual macroscopic fabrics, reinforce the opinion that quartz-rich pottery of this type is locally produced. Petrographically, there is little evidence which could refute this interpretation.
- A1.5.12 The clay used to produce most of the 12 ceramic samples is silty or sandy, containing varying amounts of mono- and polycrystalline quartz and white mica. The occurrence of arenitic sandstone inclusions of different grade (A66/2 – fine, A66/12 – coarse) in several samples indicates that much of this quartz could have come from the breakdown of a sedimentary rock. The underlying bedrock of the study area is characterised by the alternation of Carboniferous limestone and sandstone units of the Alston Formation.

(British Geological Survey 1997, Stone *et al* 2010) Quartz-rich sedimentary rocks are therefore not uncommon in the vicinity of the two sites. Petrographic analysis of the Carboniferous arenaceous rocks of this part of the northern Pennines (Dunham and Wilson 1985, 24-5) confirms them to be quartz-rich, containing clasts derived from an igneous, granitic source, and with very little material of metamorphic origin. The presence of polycrystalline quartz in many of the sherds (eg A66/9 and A66/11) and the microcline in some samples (eg A66/7) might suggest that the clay contains material derived from other sandstone sources. Dunham and Wilson (1985, 25) describe a more arkosic sandstone bed in the Three Yard Limestone outcrop, which contains polygranular metamorphic quartz.

A1 5 13 Much of the study area is covered with Pleistocene glacial till that was left by ice travelling from the west. This consists mainly of boulder clay, which ranges in composition from a gravelly or sandy deposit with a small amount of clay to a true clay without boulders or fragments of any kind (Mills and Hull 1976). The nature and origin of the clasts in these glacial deposits varies from place to place, depending on the specific ice stream that left it behind. Some contain non-local erratics from a range of sources, including the Lake District to the east, whilst the boulder clay in other areas is composed mostly of locally derived material. Unfortunately, its character has not been described in detail, since the relevant geological map (British Geological Survey 1997) has no accompanying memoir. Glacial clays have been used in this area in the past for the manufacture of bricks and tiles, including near East Layton (Mills and Hull 1976, 215). It is therefore feasible that the clay used for many of the ceramics was local boulder clay with quartz and sandstone clasts of predominantly local origin. One problem with this interpretation is the absence of limestone clasts in the clay. Limestone alternates with sandstone and outcrops in places, so locally derived glacial deposits are likely to contain clasts of both of these lithologies. An explanation could be that the material was decalcified at the surface, or alternatively, that the drift is not in fact local in origin, and derives from the erosion of the Millstone Grit Series or other sandstones. Without more data on the composition of the boulder clay in the study area or field samples, it is not possible to distinguish between these hypotheses. However, given the widespread distribution of glacial material, that covers much of the land surface in this area, and the occurrence of sandstone bedrock, it is feasible that a boulder clay source was used. Glaciofluvial and more recent alluvium, which is likely to contain significant reworked glacial material, occurs not far from SCA8 and SCA15. These might also be considered as possible sources for the clays used in the production of the ceramics.

A1 5 14 Clearly, several different, but perhaps related, clay sources were utilised for the ceramics analysed. These vary in their texture and the abundance of clasts. Samples A66/1 and A66/3 have a very fine base clay, almost devoid of inclusions, whereas samples A66/7 and A66/12 were produced from a much coarser sandy clay with abundant clasts. It is possible that a range of different related non-calcareous clay deposits could have been procured from laminated boulder clay deposits, which contain significant variation in grain size and clay/clast content. Within the eight sherds characterised by angular

voids, several different base clays were used. These could have feasibly been procured within a short distance from one another.

Al 5 15 The basalt inclusions that characterise sample A66/2 have been interpreted as deliberate tempering of crushed rock. Primary sources of basic igneous rocks do not occur in the study area, though a small surface outcrop of dolerite can be found about ten miles to the north. A possible local source of basalt might be exotic clasts in glacial deposits, such as boulder clay or gravels. Although no detailed description of the glacial material in the study area was available at the time of writing, Mills and Hull (1976, 192, 195) indicate that basic igneous rocks occur as erratics in the boulder clay of the area covered by the adjacent geological map (British Geological Survey 1969). In this case, it is possible that the vessel to which sample A66/2 belonged was produced locally, by the addition of this type of material to a base clay such as that described above. Several instances of prehistoric potters utilising specific types of erratics have been reported in the literature (*eg* Rigby 1986) and it may be that basalt was deliberately selected, crushed and added as a temper. An alternative hypothesis is that a boulder clay, containing both exotic basalt clasts and perhaps more locally derived quartz and sandstone, was used. However, the absence of exotic clasts of other compositions and the somewhat angular nature of the basalt inclusions are taken to suggest that the latter represent temper rather than naturally occurring inclusions.

Al 5 16 The now degraded angular inclusions that occur in eight out of the 12 sherds are also interpreted as temper. An alternative hypothesis could be that they were fragments of locally derived Carboniferous limestone and were naturally occurring in a glacial or alluvial deposit with locally derived clasts. Nevertheless, it is possible to rule out the possibility that they are naturally occurring, on account of their angular nature compared to the other inclusions, their larger grain size, and their occurrence in several fabrics with otherwise different clay types. Given that it is not possible to identify the nature of these mostly degraded inclusions with certainty, it is difficult to comment on the likely provenance of the material. Soluble, calcareous rock exists locally in the form of the Carboniferous limestone bedrock units that occur close to the A66. For the most part, these limestone beds are bioclastic (Dunham and Wilson 1985, 24), though replacement chert may also exist, for example in the Underset Limestone, which forms the bedrock beneath SCA15. It is not clear whether gypsum occurs in these limestone units, although it can replace calcite in carbonate rocks.

Al 5 17 Comparative thin-section analyses of other late Iron Age-early Romano-British pottery from the area include the study by Vmce (2006) of material from Piercebridge, Co Durham. Prehistoric and Romano-British ceramics, tempered with basic igneous rock, that fit the description of sample A66/2 were encountered in this study. In his macroscopic analysis of contemporaneous material from Rock Castle, Willis (1994) also records several dolerite-tempered fabrics. These also contain quartz and sandstone inclusions like sample A66/2 and the material described by Vmce (2006). Willis (1994, 30) notes that 'the frequency of sherds in dolerite tempered ware is unsurprising since this is a familiar, and now well documented,

inclusion in the Iron Age tradition pottery of the Tees lowlands and its hinterland' As in the present report, Vince (2006) interprets a glacial erratic source for the basic igneous temper

A1 5 18 At Piercebridge, Vince (2006) found the most common Romano-British 'native'-type ware to be composed of a fabric characterised by quartz silt and sand derived from sandstone. This might be considered to be equivalent to samples A66/7, A66/9, A66/11 and A66/12. Indeed, Vince (2006) suggests that they may have been produced from boulder clay or glacial lake clays, which occur in the Piercebridge area.

A1 5 19 Ceramics with a fabric equivalent to the main group of samples in the present study were not encountered by Vince (2006) at Piercebridge or by Willis (1994) at Rock Castle. However, grog temper was encountered in two macroscopic fabrics at Rock Castle. There, grog occurs with vegetable temper and dolerite temper respectively.

A1 5 20 To summarise, the thin-section petrographic analysis of the 12 Late Iron Age-early Romano-British sherds, and a comparison with both local geology and the detailed study of contemporaneous artefacts from neighbouring sites, suggests that they could have been locally produced. Possible sources for most of the raw materials have been identified. A question remains as to whether the now-degraded temper that occurs in many of the samples could have been procured nearby. However, this awaits a more positive identification of this material.

APPENDIX 2 ROMANO-BRITISH POTTERY FABRIC SERIES

- B01 Black-burnished ware Fabric 1 (Tomber and Dore 1998, 127 DOR BB1)
- O01 Orange oxidised ware some moderate sand, some gold mica, some large ironstone
- O02 Orange oxidised ware clean, soapy oxidised ware, black core
- O03 Orange oxidised ware common fairly fine sand, 0.1-0.2mm, occasional gold mica
- O04 Orange oxidised ware smooth, clean, common fine gold mica, some organics
Early Severn Valley ware (Webster 1976, Tomber and Dore 1998, 148-50 SVW OX)
- O05 Orange oxidised ware soapy, clean with some moderate sand
- R01 Pale grey rusticated ware
- R02 Dark grey reduced ware some common fairly coarse sand, 0.3mm, poorly levigated
- R03 Fine reduced ware black core, dark brown surfaces, fine sand, 0.5mm, reduced equivalent of:O02
- R04 Mid-grey reduced ware some moderate sand, 0.3mm
- W01 Soft, clean powdery whiteware
- W02 Abundant fine sandy whiteware

APPENDIX 3 SOIL MICROMORPHOLOGY

A3.1 INTRODUCTION

A3 1 1 Two soil monoliths were assessed, one (sample 201) from deposits filling the Scots Dyke ditch (12035) at SCA10 (Sections 2 3 16-17), the other (sampled 299) from ditch 14683 at SCA15 (Section 3 3 45). Field photographs and section drawings were kindly supplied by Elizabeth Huckerby and Fraser Brown of OA North.

A3.2 METHODS AND SAMPLES

A3 2 1 Monoliths 201 and 299 were sub-sampled for nine bulk analyses (Table 33), after which the monoliths were sub-sampled for soil micromorphology (five thin sections, Table 3, Pls 39-44).

A3 2 2 **Chemistry and Magnetic Susceptibility:** analysis was undertaken on the fine earth fraction (*ie* <2mm) of the samples. Phosphate-P_i (inorganic phosphate) and phosphate-P_o (organic phosphate) were determined using a two-stage adaptation of the procedure developed by Dick and Tabatabai (1977), in which the phosphate concentration of a sample is measured first without oxidation of organic matter (P_i), using 1N HCl as the extractant, and then on the residue following alkaline oxidation with sodium hypobromite (P_o), using 1N H₂SO₄ as the extractant. Phosphate-P (total phosphate) has been derived as the sum of phosphate-P_i and phosphate-P_o, and the percentages of inorganic and organic phosphate calculated (*ie* phosphate-P_i/P and phosphate-P_o/P, respectively). LOI (loss-on-ignition) was determined by ignition at 375 °C for 16 hours (Ball 1964).

A3 2 3 In addition to χ (low frequency mass-specific magnetic susceptibility), determinations were made of χ_{\max} (maximum potential magnetic susceptibility) by subjecting a sample to optimum conditions for susceptibility enhancement in the laboratory. χ_{conv} (fractional conversion), which is expressed as a percentage, is a measure of the extent to which the potential susceptibility has been achieved in the original sample, *viz* $(\chi/\chi_{\max}) \times 100.0$ (Tite 1972, Scollar *et al* 1990). In many respects this is a better indicator of magnetic susceptibility enhancement than raw χ data, particularly in cases where soils have widely differing χ_{\max} values (Crowther 2003, Crowther and Barker 1995). χ_{conv} values of $\geq 5.00\%$ are often taken as being indicative of some degree of susceptibility enhancement. A Bartington MS2 meter was used for magnetic susceptibility measurements. χ_{\max} was achieved by heating samples at 650 °C in reducing, followed by oxidising, conditions. The method used broadly follows that of Tite and Mullins (1971), except that household flour was mixed with the soils and lids placed on the crucibles to create the reducing environment (after Graham and Scollar 1976, Crowther and Barker 1995).

Context	LOI ^a (%)	Phosphate-P _i (mg g ⁻¹)	Phosphate-P _o (mg g ⁻¹)	Phosphate-P ^b (mg g ⁻¹)	Phosphate-P _i , P (%)	Phosphate-P _o , P (%)	χ (10 ⁻⁸ m ³ kg ⁻¹)	χ_{\max} (10 ⁻⁸ m ³ kg ⁻¹)	χ_{conv} ^c (%)
Monohth 201									
12098	4.04*	0.518	0.432	0.950	54.5	45.5	43.0	2970	1.45
12097	4.11*	0.615	0.594	1.21	50.9	49.1	29.4	3180	0.92
12096	4.36*	1.09	0.651	1.74*	62.6	37.4	23.7	2660	0.89
12095	3.79	1.10	0.511	1.61*	68.3	31.7	28.5	2610	1.09
Monohth 299									
14979	2.38	1.07	0.161	1.23	86.9	13.1	10.9	1390	0.78
14884	0.456	0.150	0.034	0.184	81.5	18.5	1.0	438	0.23
14885a	2.57	0.509	0.120	0.629	80.9	19.1	6.8	1880	0.36
14885b	0.801	0.146	0.038	0.184	79.3	20.7	12.6	449	2.81
14886	4.10*	0.978	0.146	1.12	87.0	13.0	129	1140	11.3*

^a LOI values highlighted indicate notably higher LOI ($\geq 4.00\%$) than the remaining samples

^b Phosphate-P values highlighted indicate likely phosphate-P enrichment

^c χ_{conv} value highlighted indicates likely magnetic susceptibility enhancement

Table 33 Analytical data

Thin			Bulk	MFT	SMT	Voids	Gravel	Clasts	Very fine	Fine	Burned
Section	Context	Depth	Sample						charcoal	charcoal	mineral
M201A	12098	0 83-0 94m	12098 201-1	A4	2b/1b/2a	25%			aaaa/aa	a	
M201B	12097	0 94-1 01m	12097 201-2	A3	2a, 1a/1b	30%			aa	a	
M201C	12096	1 01-1 12m	12096 201-3	A2	1a, 1b, 2a	35%			aa		
M201C	12095	1 12-1 52m	12095 201-4	A1	1a, 1b, 2a	35%	a-2		aa		
M299A	14979	0 09-0 11m	14979 299-1	C4	3a, 4b	25%	a-1		(aaa)	a	a-1
M299A	14884	0 11-0 145m	14884 299-2	C3	3a(4b)	15%			(aaa)		
M299A	14885a	0 145-0 16m	14885a 299-3	C2	3a, 4b	25%			aaa	aa	
M299B	14885b	0 20-0 25m	14885b 299-4	C2	3a, 4b	25%			aaa	aa	
M299B	14886	0 25-0 29(35)m	14886 299-5	C1	2a, 1c, 4a, 4b	20%	a*	aaa	aaaaa	aaa	aa
M299B	14977	0 29(35)-0 35m		B1	3a, 1c	10%			a	a*	
Thin	Context	Leached	Iron	Root	Silty	Clayey	Limpid	Fe	Fe-Mn	Broad	Broad
section		bone	fragments	traces	pans	Intercal	clay	staining	staining	burrows	excrements
M201A	12098			a	(aaa)	aaaa	a	aaaaa	a	aaaaa	aaa
M201B	12097			a*	aaaaa	aaaaa	aa	aaaaa	a	aaaaa	a
M201C	12096			a*	aaa	aaaaa	a*	aaaaa		aa	a
M201C	12095			a*	a	aaaaa	a*	aaaaa		aaa	aa
M299A	14979							aa		aaaa	
M299A	14884							(aa)		aaa	
M299A	14885a			a*	a	aaa		aaa			
M299B	14885b			a*	a	aaa		aaa			
M299B	14886	a*	a-2	a*				a*		aaaaa	
M299B	14977							a		a	

* - very few 0-5%, f - few 5-15%, ff - frequent 15-30%, fff - common 30-50%, ffff - dominant 50-70%, fffff - very dominant >70%
a - rare <2% (a*1%, a-1, single occurrence), aa - occasional 2-5%, aaa - many 5-10%, aaaa - abundant 10-20%, aaaaa - very abundant >20%

Table 34 Soil micromorphology count

A3 2 4 **Soil Micromorphology:** monoliths 201 and 299 were sub-sampled to produce 150-160mm-long samples that were impregnated with a clear polyester resin-acetone mixture (Pls 39 and 40), samples were then topped up with resin. The cured samples were then sectioned, and sub-samples chosen for 75 x 50mm-size thin-section study, ahead of manufacture by Spectrum Petrographies, Vancouver, Washington, USA (Goldberg and Macphail 2006, Murphy 1986, Pls 41-4, Table 34). When received, thin sections were further polished with 1000 grit papers and analysed using a petrological microscope under plane polarised light (PPL), crossed polarised light (XPL), oblique incident light (OIL) and using fluorescent microscopy (blue light – BL), at magnifications ranging from x1 to x200/400. Thin sections were described, ascribed soil microfabric types (MFTs) and microfacies types (MFTs), and counted according to established methods (Bullock *et al* 1985, Courty 2001, Courty *et al* 1989, Goldberg and Macphail 2006, Macphail and Cruise 2001, Stoops 2003).

A3.3 RESULTS

A3 3 1 **Chemistry and magnetic susceptibility:** the analytical results, with the key anthropogenic features of individual contexts highlighted, are presented in Tables 33 and 34. A broad overview of the individual soil properties is presented.

A3 3 2 **Organic matter (estimated by LOI)** despite the evidence of waterlogging/gleying in both monoliths, none of the contexts analysed is particularly organic-rich (maximum LOI, 4.36%). Monolith 201 appears less gleyed, but the contexts analysed have a generally higher and less variable LOI (range, 3.79–4.36%) than those from monolith 299 (0.456–4.10%). This suggests that the fills in monolith 201 were originally more organic-rich, presumably as a result of the inwash of more organic (topsoil-derived?) sediments and/or inputs of organic deposits from decaying vegetation within the ditch as the sediments accumulated. In contrast, the fills of monolith 299 would appear to be much more variable in character, with two fills (14885 and 14884) having very low LOI values (0.801% and 0.456%, respectively). Interestingly, these two fills appear to be more sandy than the other fills, and it may be that these represent inputs of more minerogenic (subsoil-derived?) sediments.

A3 3 3 **Phosphate (phosphate-P_t, P_o, P_i, P_l and P_o P)** the fills display quite marked variability in phosphate-P concentration (range, 0.184–1.74 mg g⁻¹), though none of the values recorded is especially high. The two more sandy fills from monolith 299 have the lowest values (both 0.184 mg g⁻¹), which is likely to a large extent to reflect the naturally low phosphate-retention capacity of sands. The phosphate-P concentrations are generally higher in monolith 201, and two fills (12095 and 12096) are identified (in Table 33) as showing likely phosphate enrichment (1.61 mg g⁻¹ and 1.74 mg g⁻¹, respectively). However, it should be noted that the somewhat elevated values recorded in monolith 201 are largely attributable to higher concentrations of organic phosphate (range, 0.432–0.651 mg g⁻¹, cf 0.034–0.161 mg g⁻¹ in monolith 299). Indeed, the proportions of organic phosphate recorded in

monolith 201 (phosphate-P_o P, 31.7–49.1%) are higher than are normally encountered, and this suggests that there has been only limited post-depositional decomposition/mineralisation of organic matter within these fills. The differences in phosphate-P between the two monoliths are therefore at least partly attributable to contrasts in the amounts of organic matter present.

A3.3.4 *Magnetic susceptibility (χ , χ_{max} and χ_{conv})* the most notable feature of the magnetic susceptibility data is the consistently higher χ_{max} values recorded in monolith 201 (range, 2610–3180 x 10⁻⁸ m³ kg⁻¹) than in 299 (range, 438–1880 x 10⁻⁸ m³ kg⁻¹). This contrast could simply be due to differences in the iron content of the materials washed into the two ditches – which would seem to be reflected, for example, in the much lower values recorded in the two sandy fills from monolith 299. In addition, however, χ_{max} may well have been affected by post-depositional mobilisation and leaching of iron under gleyed conditions. The lower χ_{max} values in monolith 299 could therefore equally be attributable to a loss of iron from these more heavily gleyed fills. Because of this, magnetic susceptibility data for gleyed sediments such as these need to be interpreted with caution (Crowther 2003).

A3.3.5 Under UK conditions, contexts with χ_{conv} values $\geq 5.00\%$ are often taken as being indicative of enhancement through burning. On this basis, fill 14886 at the base of monolith 299 stands out as the only fill showing likely signs of enhancement (χ_{conv} , 11.3%) – a fact that is supported by the much higher χ (129 x 10⁻⁸ m³ kg⁻¹, cf. maximum of 43.0 x 10⁻⁸ m³ kg⁻¹ in other fills) of this context. This suggests that 14886, or at least some mineralogical components within this fill, has been subject to heating/burning. Such susceptibility-enhanced material could have washed into the ditch (along with charcoal that was observed in the sample). However, in view of the magnitude of enhancement recorded, it seems more likely that the burnt soil material and charcoal were dumped in the ditch (for example, from a nearby fire).

A3.3.6 *Summary of chemical and magnetic susceptibility findings* the analytical results reveal some interesting differences between and within the two ditch-fill sequences.

- monolith 201 is more uniform in character (reflecting in part its likely derivation from a consistent parent material), generally more organic-rich, with likely signs of phosphate enrichment in fills 12095 and 12096 (though this may largely reflect the higher organic matter content), and no evidence of magnetic susceptibility enhancement,
- monolith 299 is much more variable in character (probably associated with different parent materials – for instance, topsoil- or subsoil-derived), with no evidence of phosphate enrichment, but strong evidence of burnt soil materials having been dumped in the ditch (fill 14886).

A3.3.7 *Soil micromorphology*: the five thin sections analysed contained ten contexts. Soil micromorphology counts and descriptions of 18 identified characteristics and micro-inclusions have been made (Tables 34, 35, Pls 39–62).

Microfacies type (MFT)/Soil microfabric type (SMT)	Thin section	Depth (relative depth) Soil micromorphology (SM)	Preliminary interpretation and comments
MFT A4/SMT 2b over 1b and 2a	M201A	0 91-0 985m SM heterogeneous and layered, laminated medium and coarse silty (SMT 2a, 0 980-0 985m), fine silty clay (SMT 1b, 0 92-0 980m), laminated medium and coarse silty clay (SMT 2b, 0 91-0 92m) <i>Microstructure</i> massive with burrowed and laminated microstructure, 25% voids, fine channels, vughs, closed vughs and fissures, <i>Coarse Mineral</i> as below, <i>Coarse Organic and Anthropogenic</i> rare strongly ferruginised very fine and fine root traces and root cells, occasional very fine charcoal, becoming abundant at top of thin section, <i>Fine Fabric</i> SMT 2b as SMT 2a, with abundant very fine charred organic matter, <i>Pedofeatures</i> abundant intercalations, with many broad burrow fills – ‘sedimentation’ and many microlaminated medium and coarse silty pans, <i>Amorphous</i> very abundant iron mottling (rare iron-manganese) with rare strong impregnation of root traces, <i>Fabric</i> very abundant broad and very broad (2-3mm) burrows, <i>Excrements</i> rare broad and many thin and broad excrements BD (12098) 4 4% LOI	Fill 12098 A series of bedded deposits, with very fine silty clay micaceous deposits between medium and coarse silty clayey deposits, the middle clayey deposits have been very broadly burrowed in the underlying silty sediments Silty sediment layers show silty fine laminations and sorting – with fine clay moving down-profile Both burrowing and fine rooting are present, with root traces being sometimes strongly ferruginised Occasional very fine charcoal occurs throughout, with the uppermost layer containing abundant fine charcoal <i>These sediment layers occur through muddy silting that is either fine silty clay in character or contains varying proportions of medium and coarse silt and sometimes fine sand – with phases of burrowing and rooting in between sedimentation It is possible that these variants in grain size reflect seasonal weather patterns</i>
MFT A3/SMT 2a with 1a over SMT 1a	M201B	0 985-1 06m SM heterogeneous with broad bedding – dominant SMT 1b in lower half of slide, with SMT 2a dominant upwards, with few SMT 1a <i>Microstructure</i> massive, weakly prismatic with fine channel microstructure, 30% voids, fine (0 5-1mm) moderately accommodated vertical planar voids, dominant fine channels, vughs and closed vughs, with chambers, <i>Coarse Mineral</i> C F, as below, but with few fine sand and no gravel, <i>Coarse Organic and Anthropogenic</i> trace amounts of possible ferruginised root traces (very abundant?), occasional very fine charcoal and rare fine charcoal, <i>Fine Fabric</i> as below, <i>Pedofeatures</i> very abundant textural intercalations, as below, but with rare (occasional in upper slide) limpid but poorly birefringent clay void coatings, <i>Amorphous</i> as below, but with stronger iron impregnations and rare likely iron-manganese impregnations, including concentric variants, with very abundant traces of fine rooting?, broad burrows also picked out, <i>Fabric</i> very abundant broad burrows, <i>Excrements</i> rare broad and thin excrements BD (12097) 4 11% LOI	Fill 12097 Thin section was taken across boundary between clayey and upwards medium and coarse silty clay sediments, which include a small proportion of fine sand Occasional very fine charred organic matter and rare fine charcoal occurs throughout As in 12096-5, textural intercalations dominate, with additional fine limpid but poorly birefringent clay also being deposited as infills Iron staining is very abundant (with rare iron-manganese impregnations) – seemingly often to be picking out root channels and broad burrows The context shows a relatively high %LOI <i>Two variations in the muddy sedimentation of this ditch are recorded, purely a very fine silty micaceous clay with, overlying it, medium and coarse silty clay and clayey sediments containing fine sand The sediments are slightly more very fine and fine charcoal-rich compared to the sediments below Fine rooting and broad burrowing affected the sediments, as shown by iron and iron-manganese staining</i>

<p>MFTA2/SMT 1a, 1b and 2b over MFTA1/SMT 1a, 1b and 2b</p>	<p>M201C</p>	<p>1 09-1 165m SM heterogeneous, with dominant SMT 1a, frequent 1b and very few 2a <i>Microstructure</i> fine prismatic with patches of laminated, 35% voids, medium (1-3mm) moderately accommodated vertical planar voids, fine channels, vughs and closed vughs, with chambers, <i>Coarse Mmeral</i> C F Limit at 10pm), SMT 1a 40-60 60-40, SMT 1b 0 100, SMT 2a 85 15, generally moderately well-sorted coarse silt to fine sand-size quartz, quartzite, feldspar, with mica (unweathered examples up to 750µm long – coarse sand-size), very few gravel size (9mm) fine sandstone rock fragments, <i>Coarse Orgamc and Anthropogenic</i> trace amounts of root traces and fine organic fragments, now ferruginised, occasional very fine charcoal, <i>Fme Fabric</i> SMT 1a speckled and dotted, greyish brown (PPL), moderate interference colours (open to close porphyric, speckled with grano- and vo-striate b-fabric, XPL), pale greyish brown with dark brown-orange mottles (OIL), weakly humic, stained with occasional very fine charred OM inclusions, and examples of amorphous OM inclusions, <i>Pedofeatures Textural</i> very abundant intercalations and matrix void coatings (closed vughs), laminated fine medium and coarse silty clay pans, with burrows showing collapsed structures (closed vughs and intercalations) and channel infills, many 1-3mm-thick silty pans (marking the boundary between 12096 and 12097, also 5mm-thick layer of fine sand-rich clayey sediment at this junction), rare very fine limpid clay void coatings, <i>Amorphous</i> very abundant moderately diffuse ferruginous impregnations 1-2mm in size, rare traces of ferruginised plant remains/roots, <i>Fabric</i> many broad (2-3mm) burrows (some showing later collapsed structure) in 12095, <i>Excrements</i> rare broad mamilated excrements – showing partial collapse in 12095, rare traces of very thin (50pm) organo-mineral excrements BD (12096) 4 36% LOI, 1 74mg g⁻¹ phosphate-P BD (12095) 1 61mg g⁻¹ phosphate-P</p>	<p>Fill 12096 over 12095 Very clayey micaceous and very fine silty sediments with variable quantities of included fine sand and/or coarse silt, and occasional very fine charcoal 12095 includes two gravel-size fine sandstone clasts Very abundant matrix intercalations and associated closed vughs throughout, with very fine impure clay micro-panning and channel infilling Medium and coarse silty panning and sandy inclusions more common in 12096, while broad burrows and broad mamilated excrements (showing some structural collapse) more common in 12095 Both contexts show phosphate enrichment, with 12096 showing a higher organic content (%LOI) 12095 – <i>probably rapid ditch silting under wet conditions (standing water and slurry inwash), with inclusion of two gravel-size fine sandstone clasts and unweathered coarse mica Presumably burrowing by earthworms took place at a dry time of the year before renewed wet and muddy conditions resumed (and earthworm excrements started to collapse) The ditch contained standing water at times, hence micro-panning, and amorphous iron staining (mottling), which may be associated with phosphate enrichment</i> 12096 – <i>very much as 12095, but sedimentation included more fine sand and coarse silt, and wet conditions apparently persisted, because much less biological activity is recorded The sediment is similarly enriched in phosphate and is a little more humic It is possible that the sedimentation of 12095 and 12096 – as seen in thin section M201 – occurred during just a few years</i></p>
---	--------------	--	--

MFT C4/SMT 3a below mainly 4b	M299A	<p>0 085-0 16m 0 085-0 11m (14979)</p> <p>SM heterogeneous, with dominant SMT 3a and frequent 4b becoming more common upwards <i>Microstructure</i> massive, once-fine and coarse laminated (3a and 4b), burrowed, 25% voids, with channels, vughs and simple packing voids, <i>Coarse Mineral</i> as below, with 16mm+-size fine sandstone rock fragment, <i>Coarse Organic and Anthropogenic</i> rare very fine charcoal, becoming many upwards, with trace amounts of medium (2mm) charcoal, and with burrowed-in examples of coarse wood charcoal (7mm), example of 16mm+-size fine sandstone rock fragment with rubefied iron staining (burned), <i>Fine Fabric</i> as below, <i>Pedofeatures Textural</i> occasional weakly-formed impure clay intercalations (associated with burrows), <i>Amorphous</i> rare weak iron-staining – eg around coarse wood charcoal and upper microfabric (4b), <i>Fabric</i> many broad (2-3mm), very broad (30mm) slumping(?)</p>	<p>Fill 14979</p> <p>Laminated clean coarse silt and fine sands, with burrowed fine layers of fine charcoal-rich clayey sediment Burrowed coarse (7mm) charcoal and 16+-mm-size burned fine sandstone fragments occur, as upwards more fine-charcoal-rich sediment dominates (see LOI) Much broad burrow mixing</p> <p><i>As below, with variations in wash of coarse silt and fine sands, and more fine charcoal and clayey material, with fine charcoal-rich sediment becoming dominant upwards alongside examples of coarse charcoal and burned sandstone</i></p>
MFT C3/SMT 3a(4b)		<p>0 11-0 145m (14884)</p> <p>SM weakly heterogeneous, with very dominant SMT 3a, with very few SMT 4b (burrows and laminae) <i>Microstructure</i> massive and finely laminated (0.5-1mm), becoming 1-3mm upwards, 15% voids, vughs and fine channels, simple packing voids, <i>Coarse Mineral</i> C F, as 3a, <i>Coarse Organic and Anthropogenic</i> rare overall, with many very fine charcoal in uppermost 0.2mm of laminae, <i>Fine Fabric</i> as SMT 3a and 4b, <i>Pedofeatures Amorphous</i> weak iron-staining of upward fining clayey laminae, <i>Fabric</i> rare thin (1mm) and many broad (2-3mm) burrows</p>	<p>Fill 14884</p> <p>Series of finely laminated upward-fining (clean) coarse silts and fine sands, with iron-stained (clayey) and charcoal-rich uppermost layers Mainly broad burrowing, introducing 14979 material</p> <p><i>Finely laminated upward fining leached coarse silt and fine sands, with associated fine charcoal-rich laminae in slightly clayey and iron-enriched uppermost layers Wash deposits</i></p>
MFT C2/SMT 3a, 4b		<p>SM common SMT 3a and 4b, upward-fining <i>Microstructure</i> massive, laminated (0.5-1.00mm, 1-6mm), with fine channel, 25% voids, fine channels, and closed vughs, <i>Coarse Mineral</i> well-sorted coarse silt, fine channels, and closed vughs, <i>Coarse Organic and Anthropogenic</i> many fine charcoal (maximum 1mm), <i>Fine Fabric</i> as SMT 3a and 4b with variable C F, 90 05-30 70, <i>Pedofeatures Textural</i> many intercalations and 1mm-size void dusty clay infills, <i>Amorphous</i> abundant iron-staining of clayey laminae and infills, <i>Fabric</i> occasional 0.5-1mm thick burrows</p> <p>BD (14979) 2.38% LOI</p> <p>BD (14884) 0.456% LOI</p> <p>BD (14885a and b) 2.57% and 0.801%, respectively</p>	<p>Fills 14885a and 14885b</p> <p>Finely (0.5-1mm) and moderately (1-6mm) laminated coarse silt and fine sands, with weakly humic clayey laminae, some with many fine charcoal (see LOI) Laminae show upward fining into clayey laminae, with infilling of some voids with dusty clay associated with intercalations Upper clayey laminae are iron-stained Fine rooting also noted</p> <p><i>Upward fining sequence of coarse silty and fine sandy laminae, developing over clayey and fine charcoal-rich material - laminated variant of 14886 (?), becoming less charcoal-rich, with clay becoming iron-stained</i></p>

MFT C1/SMT 2a, 4a, 4b and 1c	M299B	<p>0 235-0 31m 0 25-0 29(35)m (14886) SM very heterogeneous, with variants of SMT 2a, 4a, 4b and 1c <i>Microstructure</i> massive with fine channel, 20% voids, fine channels, vughs and complex packing voids, <i>Coarse Mineral</i> C F, SMT 4a and 4b, 60 40, moderately poorly sorted with well-sorted coarse silt and fine sand, with very coarse sand-size and gravel-size fine sandstone rock fragments and inclusions (clayey clasts, iron-stained clay – from 201-like material), <i>Coarse Organic and Anthropogenic</i> trace amounts of roots – some ferruginised, rare trace of very fine leached bone, very abundant, mainly fine charcoal (with few 2-3mm, maximum 8mm), occasional rubefied mineral grains, two possible examples of iron fragments (with iron-stained margins - hypocoatings), <i>Fine Fabric</i> SMT 4a blackish (PPL), isotropic (open porphyric, undifferentiated b-fabric, XPL), black (OIL), humic, SMT 4b speckled and dotted darkish brown (PPL), low interference colours (open to close porphyric, speckled b-fabric, XPL), grey to brown (OIL), weakly humic stained, with rare to abundant charred organic matter, phytoliths present, <i>Pedofeatures Amorphous</i> rare example of ferruginised root trace, <i>Fabric</i> very abundant thin and broad to very broad burrows</p>	<p>Fill 14886 Very heterogeneous mixture of very fine charcoal-rich clayey and sandy soils, with blackened fragments of humic sands (Ah horizon soil?), sand and clay clasts (as in M201?), with many fine charcoal (2-3mm, maximum 8mm), occasional fine rubefied mineral material, two examples of iron fragments (staining surrounding fine soil) and traces of fine leached bone (one very small concentration) Much burrowing and occasional rooting observed, one burrow is coarse silt infilled Markedly anthropogenic humic (see also LOI) fill that has been strongly burrowed An enigmatic mixture of ditch(?) and humic topsoil (Ah) clasts that show many indications of burning (rich in charcoal, and rubefied mineral grains – note also strongly enhanced magnetic susceptibility), two small iron fragments occur In addition to suggesting the deposit is the result of infilling by a cultural 'soil' – trampled floor deposits(?), the amount of charred soil inclusions may indicate burning of humic sods to produce a certain amount of 'peat ash'</p>
MFT B1/SMT 3a, 1c		<p>0 29(35)-0 31(0 35)m (14977) SM moderately heterogeneous, with very dominant SMT 3a and frequent SMT 1c (and variants) <i>Microstructure</i> massive, bedded, 10% voids, fine channels and vughs, simple packing voids, <i>Coarse Mineral</i> C F, SMT 3a, 95 05, very well-sorted beds of fine sand-size quartz and well-sorted coarse silt (at base of thin section), C F SMT 1c, 05-15 95-85, mica-dominated, <i>Coarse Organic and Anthropogenic</i> rare charcoal (maximum 2mm) and trace amounts of mbefied mineral material, <i>Fine Fabric</i> SMT 1c speckled dark brown to blackish brown (PPL), moderately low interference colours (open porphyric, speckled (crystallitic-mica) b-fabric, XPL), orange to dark brown (OIL), rare to very abundant charred fine OM, SMT 3a pale greyish brown, fine speckled (PPL), very low interference colours (single grain, coated grain, close porphyric, speckled b-fabric, XPL), very pale grey (OIL), trace of very fine charred OM, <i>Pedofeatures Textural</i> rare trace of poorly birefringent clay void infills – including fine charcoal?, <i>Amorphous</i> rare trace of iron void coatings, associated with clay-lined voids, <i>Fabric</i> rare very broad (6mm) burrows BD (14886) 4 10% LOI, 11 3% χ_{conv}</p>	<p>Fill 14977 Generally bedded and well-sorted clean fine quartz sand and coarse silts, with burrow fills and mixing from 14886 above, minor clay and iron void coatings <i>Ditch fill of fine and coarse 'siltng', by leached sands and coarse silts, some post-depositional burrow mixing and inwash from above</i></p>

Table 35 Soil micromorphology descriptions and preliminary interpretation

- A3 3 8 *Monolith 201 (SCA10)* fills 12096 over 12095 (M201C) are both very clayey micaceous and very fine silty sediments, with variable quantities of included fine sand and/or coarse silt, and occasional very fine charcoal. Fill 12095 includes two gravel-size fine sandstone clasts (Pls 41, 45, 46). There are very abundant matrix intercalations and associated closed vughs throughout, with very fine impure clay micro-panning and channel infills. Medium and coarse silty panning and sandy inclusions are more common in 12096, while broad burrows and broad mamillated excrements (showing some structural collapse, PI 47) are more common in 12095. Both fills show phosphate enrichment, with 12096 showing a higher organic content (Table 33).
- A3 3 9 Fill 12095 probably results from rapid ditch silting under wet conditions (standing water and slurry inwash), with the inclusion of two gravel-size fine sandstone clasts and unweathered coarse mica. The gravel clasts are anomalous in this clayey sediment. Presumably burrowing by earthworms took place at a dry time of the year, before renewed wet and muddy conditions resumed (and earthworm excrements started to collapse). The ditch probably contained standing water at times, hence micro-panning, and amorphous iron staining (mottling) which may be associated with phosphate enrichment (see Pls 48, 49).
- A3 3 10 Fill 12096 is very much like 12095, but sedimentation included more fine sand and coarse silt, and wet depositional conditions apparently persisted for longer, because much less biological activity is recorded. The sediment is similarly enriched in phosphate and is a little more humic. It is possible that the sedimentation of 12095 and 12096 – as seen in thin section M201C – occurred during just a few years.
- A3 3 11 Thin section M201B (fill 12097) was taken across a boundary between clayey, and upwards, medium and coarse silty clay sediments, which include a small proportion of fine sand. Occasional very fine charred organic matter and rare fine charcoal occur throughout. As in 12096 and 12095, textural intercalations dominate, with additional fine limpid but poorly birefringent clay also being deposited as infills. Iron staining is very abundant (with rare iron-manganese impregnations), seemingly often to pick out root channels and broad burrows (Pls 48, 50). The fill shows a relatively high organic content and χ_{\max} – the last reflecting iron staining.
- A3 3 12 This thin section of fill 12097 records two variations in the muddy sedimentation of this ditch: first, a very fine silty micaceous clay with, overlying it, medium and coarse silty clay and clayey sediments containing fine sand. The sediments are slightly more very fine and fine charcoal-rich compared to the sediments below. Fine rooting and broad burrowing affected the sediments, as shown by secondary iron and iron-manganese staining.
- A3 3 13 Fill 12098 (M201A) is composed of a series of bedded deposits, with very fine silty clay micaceous sediments between medium and coarse silty clayey deposits. The middle clayey layers have been very broadly burrowed into the underlying silty sediments (Pls 42, 51, 52). Silty sediment layers show silty fine laminations and sorting, with fine clay washing down-profile. Both

burrowing and fine rooting are present, with root traces being sometimes strongly ferruginised. Occasional very fine charcoal occurs throughout, with the uppermost layer containing abundant fine charcoal.

A3 3 14 These sediment layers in fill 12098 formed through muddy silting that is either a fine silty clay in character or contains varying proportions of medium and coarse silt and sometimes fine sand, and with phases of burrowing and rooting in between sedimentation episodes. It is possible that these variations in grain size reflect seasonal weather patterns.

A3 3 15 *Monolith 299 (SCA15)* fill 14997 (M299B lower) is a generally bedded and well-sorted sediment composed of clean fine quartz sand and coarse silts, with burrow fills and mixing from 14886 above (Pls 40, 44). Minor clay and iron void coatings were noted. This is a ditch fill developed through fine and coarse 'silting' of leached sands and coarse silts. The deposit was affected by some post-depositional burrow mixing and inwash from above.

A3 3 16 Fill 14886 (M299B upper) is a very heterogeneous mixture of very fine charcoal-rich clayey and sandy soils (Pls 39 and 43). It contains blackened fragments of humic sands (Ah horizon soil?), sand and clay clasts (as in M201?), with many fine and medium charcoal (2-3µm, maximum 8µm), occasional fine mbedded mineral material, two examples of iron fragments (which stain the surrounding fine soil) and traces of fine leached bone (one very small concentration, Pls 53-7). Much burrowing and occasional rooting was observed, and one burrow is infilled with clean coarse silt.

A3 3 17 Compared to 14997, 14886 is a markedly anthropogenic and relatively humic (see also LOI) fill that has been strongly burrowed. There is an enigmatic mixture of ditch (?), gleyed Bg horizon (?) and humic topsoil (Ah) clasts that show many indications of burning, along with other included material, such as the amount of charcoal and mbedded mineral grains (note also the strongly enhanced magnetic susceptibility). Two small iron fragments occur which may also contribute to the enhanced magnetic susceptibility. In addition to suggesting that the deposit is the result of ditch infilling by cultural 'soil', for example, trampled occupation deposits (?), the amount of charred soil inclusions may indicate burning of humic sods to produce what is known as peat ash.

A3 3 18 Fill 14885 (M299-base) is composed of finely (0.5-1.0mm) and moderately (1-6mm) laminated coarse silt and fine sands, with weakly humic clayey laminae, some with many fine charcoal (see Table 33, %LOI). Laminae show upward fining into clayey laminae (Pls 43, 58-60), with infilling of some voids with dusty clay associated with intercalations. Upper clayey laminae are iron-stained. Fine rooting was also noted.

A3 3 19 Lower fill 14885 is an upward fining sequence of coarse silty and fine sandy laminae, developing over clayey and fine charcoal-rich material (which is a possible laminated variant of 14886). It becomes less charcoal-rich upwards, with clay becoming iron-stained.

- A3 3 20 Fill 14884 (M299–middle) forms a series of finely laminated upward-fining (clean) coarse silts and fine sands, with iron-stained (clayey) and charcoal-rich uppermost layers. Mainly broad burrowing introduces 14979 material from above (Pl 43). Fill 14884 is made up of finely laminated upward fining leached coarse silt and fine sands, with associated fine charcoal-rich laminae in slightly clayey and iron-enriched uppermost layers. These are also ditch mwash deposits.
- A3 3 21 Fill 14979 (M299–top) is composed of laminated clean coarse silt and fine sands, with burrowed fine layers of fine charcoal-rich clayey sediment. Examples of burrowed-in coarse (7mm) charcoal and 16+mm-size burned fine sandstone fragments occur, as, upwards, more fine charcoal-rich sediment dominates (see Table 33, %LOI, Pls 39, 43, 61-2). There is much broad burrow mixing.
- A3 3 22 Fill 14979 is similar to 14884, below it, with variations in wash of coarse silt and fine sands, and more fine charcoal and clayier material, with fine charcoal-rich sediment becoming dominant upwards, alongside examples of coarse charcoal and burned sandstone. The latter coarse materials are more typical of fill 14797.

A3.4 DISCUSSION

- A3 4 1 **Local soils:** local soils are grouped into the Brickfield 2 soil association – mainly Cambic stagnogley soils that are formed on drift from Mesozoic sandstone and finer-grained rocks (Jarvis *et al* 1983). It is clear, however, that the fills of the two ditches analysed are quite different in terms of their grain size, monolith 201 sampling a fine clayey fill, whereas monolith 299 is mainly coarse silt to fine sand in character. This strong contrast in fill type can perhaps be explained by suggesting that monolith 299 reflects immediate on-site activity, whereas 201 (from Scots Dyke) does not.
- A3 4 2 **Scots Dyke fill, monolith 201** this is composed of many muddy clayey silting episodes, with rare mwash of gravel (two pieces) and occasional coarse silt and fine sand. It can be suggested that these coarser elements reflect the local geology and soils through which the dyke was cut, but that the dominantly clayey fill derives from more heavy textured soils upslope (?). This is indicated by the field photographs (kindly supplied by Eliabeth Huckerby and Fraser Brown) that show the sloping nature of the dyke, the sampled area is seemingly acting as a 'receiving site'.
- A3 4 3 Presumably clayey soil, mobilised by ramstorms upslope, washed downslope along the dyke into the location sampled. It often arrived as muddy slurry, and filled both coarse channels and voids, and sometimes partially slaked earlier-formed earthworm excrements. There seem to have been multiple cycles, with periods of biological working in between. These may broadly represent 'seasonal' episodes, with 'dry' summer periods of biological activity, and 'wetter' winter periods of clayey silting. The deposits are also relatively humic and enriched in phosphate, which may imply anthropogenic inputs, possibly from stock, as the proportion of organic phosphate is noticeably

high. Hypothetically, some of the muddy fills could have occurred through animal trampling. No dung fragments were found, however. Organic and phosphate enrichment were noted at the ditch at prehistoric Battlesbury, Wiltshire, which was tentatively identified as resulting from cess inputs (Macphail and Crowther 2008). No evidence of cess inputs was found in monolith 201, though.

A3 4 4 *Dutch fill, monolith 299* laminated (waterlain) fine sandy and coarse silty fills (eg 14997) seem to alternate with major (14886) and minor charcoal-rich fills that are either finely laminated or biologically worked (14886, Pls 39-41, 52-4). These ditch fills probably reflect the use of the site, which again may have seasonal characteristics. The laminated deposits were probably formed after rainstorms eroded the coarse silt and fine sand from the exposed soils in the sides of the ditch, and when standing water existed for a while, examples of fine sandstone clasts are present at the site. These deposits are in stark contrast to the anthropogenic character of 14886. This is humic, very charcoal-rich, and includes rare examples of leached bone, metal (iron?) fragments, burned humic topsoil and fine mbedded mineral inclusions. This humic and 'burned' character was also suggested from chemistry and the strongly enhanced magnetic susceptibility (4.10% LOI, 11.3% χ_{00nv}). It is also biologically worked, suggesting that the fill was deposited under aerobic 'dry' conditions, before the next episode of rainstorm(s) generated coarse silty and fine sandy laminated sedimentation.

A3 4 5 The nature of the anthropogenic fill can probably best be described as resulting from fuel ash, where both wood and peaty turf were employed as fuel. The use of minerogenic turf/peat as fuel is well recorded in Scotland from fuel ash-rich middens, as is its occurrence in manured soils (Adderley *et al* 2006, Carter 1998a, Carter 1998b, Simpson 1997). Sometimes this material is included as fine wash, or as coarse material in fill 14979 (although only a very small amount of this was studied in M299A), including burned sandstone (Pls 39, 55-6). The apparent alternation between charcoal-rich deposits, that are biologically worked, and laminated coarse silts and fine sands may again suggest seasonal use of the site. As only one location was studied, this suggestion must remain tentative, however.

A3.5 CONCLUSIONS

A3 5 1 The study of five thin sections and nine bulk samples from monolith samples suggested that the anomalous clayey fill of the Scots Dyke (monolith 201) in an area of coarse silt and fine sands resulted from muddy slurries washing along the dyke downslope from an assumed more clayey soil area. The fill is relatively enriched in organic matter and phosphate, although no exact phosphate source(s) has been identified. In contrast, monolith 299 more probably reflects local inwash of coarse silty and fine sandy soil, which was often deposited under ephemeral standing water conditions. Inwash of these 'clean' sediments seems to have alternated with charcoal, burned turf and soil deposits, which are of probable turf-based fuel-ash origin, and which were biologically worked. These cycles of deposition may possibly reflect seasonal occupation/activity, but this hypothesis remains tentative.

APPENDIX 4 ARCHAEOMAGNETIC DATING

A4.1 SAMPLE COLLECTION AND PREPARATION

A4 1 1 In total, 28 oriented specimens were collected for archaeomagnetic dating from a sedimentary fill in the Scots Dyke ditch (12035) at SCA10 (NZ 195 063, $\phi = 54.0453^\circ$, $\lambda = -0.7006^\circ$). These specimens were collected on 1st August 2006, by carefully inserting 20 x 20mm plastic pots into the north-facing section, trying to produce as little sediment disturbance as possible. The left to right tilt of the top-surface of the plastic pots was kept as close as possible to zero, controlled by a spirit level attached to a specially designed insertion plate. The dip of the front face of the pot was measured with an inclinometer to an accuracy of $\pm 0.5^\circ$. The insertion direction was measured with a magnetic compass. With these two measurements, it is possible to determine the *in situ* direction of the sediment magnetisation from the specimen magnetisation.

A4 1 2 The now-oriented specimens were removed from the sediment, immediately capped with a plastic lid, sealed by tape and kept in a fridge once back at Lancaster University, in order to minimise any changes in water content. Specimens were coded 'SC' and with a two-digit number denoting the depth below the subsoil surface.

A4 1 3 Two specimens (SC27 and SC30) came from 12100 (a modern subsoil horizon), and 26 more came from the sedimentary horizons between the base of 12100 and top of the primary fill of the ditch (12094), a coarse-grained silt with pebbles (Fig 70). The upper part of the profile (fills 12099, 12098, and 12097) was composed of beige-brown silty sand. It was informally labelled as section A and included 13 specimens (SC33 to SC64) between depths of 0.33m and 0.64m below the subsoil surface. The lower part of the profile (fills 12096 and 12095) was finer-grained, composed of darker-coloured clayey silt. Horizon 12096 was possibly a palaeosol. This part of the profile was labelled as section B and it included 13 specimens (SC67 to SC98) between depths of 0.67m and 0.98m below the subsoil surface.

A4.2 ARCHAEOMAGNETIC PROCEDURES AND RESULTS

A4 2 1 The direction and strength of natural magnetisation of the specimens were measured at the CEMP, Lancaster University, using an AGICO JR6A spinner magnetometer. Low speeds were used on the JR6A in order to avoid disturbance to the specimens.

A4 2 2 The low-field magnetic susceptibility was measured on a Bartington MS2 susceptibility meter at two frequencies, low (0.46kHz giving χ_{LF}) and high (4.6kHz giving χ_{HF}). The difference between these two, the frequency-dependent magnetic susceptibility (χ_{FD} %), was calculated as a percentage of χ_{LF} . This is a measure of the abundance of superparamagnetic magnetite (ultra-fine magnetite $< \sim 0.03\mu\text{m}$) in the samples, which is commonly a good indicator of topsoil magnetic enhancement, or, in this case, sediment derived from topsoil (Dearing 1999).

A4 2 3 Magnetic cleaning techniques (demagnetisation) were applied to the specimens. These techniques attempt to isolate a stable magnetisation from each specimen, and take the most time and effort in the whole dating procedure. This is always necessary with natural specimens, since sediment magnetisations are to a varying extent time-dependent, and acquire additional 'magnetic noise' with increasing time. Further details about the methodology, and archaeomagnetic background, can be found in *Section A4 5*, and in Lmford (2004, 2006).

A4 2 4 **Magnetic properties:** Table 36 lists the values of the Natural Remanent Magnetisation (NRM), the χ_{LF} , χ_{FD} %, and the Koengsberger factor Q_{NRM} of the specimens. The Q_{NRM} is the ratio between the NRM and the induced magnetisation in a 0.05mT field, which is an indication of the nature and the stability of the NRM of the specimens (Fig 71).

Specimen	NRM (mA/m)	χ_{LF} ($\times 10^{-6}$ SI)	χ_{LF} % (%)	Q_{NRM}	ChRM		
					D (°)	I (°)	Range
SC27	4.5	172.8	10.7	0.67	12.6	61.0	12-23 mT
SC30	4.7	170.3	10.4	0.71	—	—	
SC33	11.2	302.8	9.8	0.95	355.0	68.8	10-25 mT
SC36	10.7	270.3	9.0	1.01	3.0	70.3	12-23 mT
SC39	8.0	224.0	9.3	0.92	350.1	71.1	12-23 mT
SC41	8.5	247.8	9.4	0.88	0.8	70.1	9-23 mT
SC43	13.0	400.3	9.2	0.83	7.4	72.7	9-23 mT
SC46	17.3	494.0	9.0	0.89	357.8	73.3	12-23 mT
SC49	21.5	536.5	9.1	1.02	356.4	70.4	9-23 mT
SC51	14.1	327.8	9.0	1.09	2.4	65.7	12-23 mT
SC54	14.4	316.5	8.6	1.16	4.3	69.6	10-25 mT
SC56	9.1	206.5	7.9	1.14	9.1	63.2	12-23 mT
SC59	19.6	392.8	8.4	1.27	—	—	
SC61	11.3	241.5	8.8	1.20	11.6	71.5	12-23 mT
SC64	17.1	316.5	9.3	1.38	8.5	63.4	9-23 mT
SC67	15.3	276.5	8.4	1.42	352.8	67.3	9-23 mT
SC70	13.3	260.3	8.5	1.31	1.1	71.8	9-23 mT
SC72	7.6	192.8	7.8	1.02	355.7	68.8	12-23 mT
SC74	16.5	360.3	8.3	1.17	3.1	66.7	10-25 mT
SC75	15.8	356.5	7.8	1.13	357.6	72.7	9-23 mT
SC77	20.0	364.0	8.2	1.40	—	—	
SC80	13.4	276.5	8.7	1.24	352.3	77.6	9-23 mT
SC82	15.1	266.5	10.4	1.45	354.3	70.6	9-23 mT
SC86	12.8	250.3	8.9	1.31	358.4	67.0	9-23 mT
SC88	16.7	324.0	8.4	1.32	357.9	67.1	9-23 mT
SC90	13.7	291.5	8.5	1.21	358.4	67.8	10-25 mT
SC93	11.3	250.3	8.2	1.16	2.6	67.3	9-23 mT
SC96	7.3	181.5	7.8	1.04	358.1	73.5	12-23 mT

D = declination (not variation corrected) I = inclination of the ChRM components. D I pairs indicated in bold were not used in the final mean directions. Range is the alternating field demagnetisation range over which the fit of the ChRM principal component was obtained.

Table 36 Values of the Natural Remanent Magnetisation (NRM), the χ_{LF} , χ_{FD} %, and the Koengsberger factor Q_{NRM} of the specimens

A4 2 5 Three zones with somewhat distinct magnetic properties (Table 37) can be distinguished in the data

- a) The uppermost two specimens in 12100, the modern subsoil (specimens SC27, SC30), have low values of the NRM and χ_{LF} (Fig 71) The Koenigsberger factor Q_{NRM} is lowest (0.7), and χ_{FD} % is largest, with values of 10.4% and 10.7%. These χ_{FD} % values are close to the maximum values of 12-14% for modern UK soils (Walden *et al* 1999) and probably reflect both the *in situ* production of fine-grained ferrimagnetic grains from accumulation in the overlying soil, as well as original sediment derivation from topsoil (Hounslow and Chepstow-Lusty 2004) This made 12100 unsuitable for archaeomagnetic dating
- b) Section A (specimens SC33-SC64) has high NRM and χ_{LF} values Q_{NRM} increases with depth from 0.8-0.9 to 1.2, and χ_{FD} % decline with depth (Fig 71)
- c) Section B (SC67-SB96) also has high NRM and χ_{LF} values It also has the highest Q_{NRM} values, between 1.2 and 1.45 There is no indication from χ_{FD} % in deposit 12096 that this represents a substantial palaeosol, it is probable that this level is an immature palaeosol, without magnetic enhancement

Region	N_s	NRM (mA/m)	χ_{LF} ($\times 10^{-6}$ SI)	χ_{LF} % (%)	Q_{NRM}
subsoil (SC27, SC30)	2	4.6	172	10.5	0.69
section A (SC33-64)	13	13.5	329	9.0	1.06
section B (SC67-96)	13	13.8	281	8.5	1.25

N_s = number of specimens

Table 37 Mean volume-specific magnetic parameters for the three 'magnetic zones' of the Scots Dyke profile

A4 2 6 The mean values of NRM, χ_{LF} and χ_{LF} % are very similar in sections A and B The frequency-dependent magnetic susceptibility is quite high throughout (8-10%) and probably reflects the fact that a large part of the sediment fill was derived from topsoils surrounding the ditch The lower values of Q_{NRM} in section A, especially towards its top (Fig 71), are due to

- the greater presence of fine-grained, superparamagnetic (SP) ferrimagnetic grains, which contribute to the total magnetic susceptibility but not to the total remanence,
- the less effective acquisition of depositional remanence in the coarser, sandier sediments of section A (*cf* Dunlop and Ozdemir 1997)

A4 2 7 The properties of the isothermal remanent magnetisation (IRM) of four specimens, SC33, SC54, SC74, and SC90, were additionally studied in order to elucidate the nature of their mineral magnetic assemblages (Fig 72) The specimens were magnetised in seven fields using pulse and DC electromagnets The numerical values of the IRM parameters and the various ratios are shown in Table 38

Specimen	Depth	IRM 100mT	IRM 300mT	IRM 1000mT	IRM ₁₀₀ / SIRM	IRM ₃₀₀ / SIRM	SIRM/ χ_{LF}
	m	mA/m	mA/m	mA/m	%	%	E+3 A/m
SC33	0.33	1380	1470	1576	88	6.7	5.2
SC54	0.54	1386	1479	1601	87	7.6	5.1
SC74	0.74	1243	1336	1435	87	6.9	4.0
SC90	0.90	965	1051	1149	84	8.5	3.9

Table 38 Numerical values and ratios of the IRM parameters of four representative specimens from the Scots Dyke profile. Saturation IRM (SIRM) is the value of IRM at 1000mT.

- A4.2.8 All four specimens have very similar modes of IRM acquisition. They acquire some 84-88% of the saturation IRM (SIRM) by 100mT and reach near saturation by 300mT, which indicates the dominance of ferrimagnetic minerals. Another, probably ferromagnetic, component is responsible for 7-9% of the SIRM, acquired in fields above 300mT (IRM₃₀₀/SIRM is the % of 'hard' IRM, acquired above 300mT). The ratio of the saturation remanence versus the magnetic susceptibility, SIRM/ χ_{LF} , is also very similar for all four specimens, ranging from 3.0 to 5.2. Such low values are characteristic for (titano) magnetites (and/or maghemites) and not for greigite or other iron sulphide minerals (Peters and Dekkers 2003).
- A4.2.9 The low values of SIRM/ χ_{LF} and the relatively low values of Q_{NRM} in both A and B sections exclude the ferrimagnetic mineral greigite (or other iron sulphide minerals) as a possible significant contributor to the natural magnetic remanence of the Scots Dyke sediments. Their NRM is most probably not chemical, due to authigenic, *in situ*-formed greigite, but depositional (or post-depositional) in nature (DRM or pDRM). This means that it must have been acquired soon after the formation of the sediment. This contrasts with other documented ditch-fills, which can be greigite-dominated (Linford *et al* 2005).
- A4.2.10 **Magnetic directional characteristics:** regardless of the differing magnetic parameters along the section, the NRM directions throughout the profile were tightly clustered, with inclusive inclinations varying between 60° and 70°, and declinations between 350° and 10° (Fig 73).
- A4.2.11 Several representative specimens were demagnetised with alternating magnetic field in eight steps up to 50mT, using a Molspin AF demagnetizer. Based on their demagnetisation characteristics, the rest of the collection were then AF demagnetised in three to four steps.
- A4.2.12 The Characteristic Remanent Magnetization (ChRM), as evident by a straight line on the Zijderveld plots (Fig 74), was revealed as 10-25mT or 9-23mT for the specimens from section A and B respectively. Figure 74 shows representative demagnetisation characteristics for specimens SC54 and SC74 from sections A and B, respectively (The numerical data of these two specimens are also listed in Tables 39 and 40). Small viscous overprints were removed by 5-10mT cleaning. These overprints are probably field and laboratory viscous magnetisations. Demagnetisation in fields higher than ~10mT revealed a single magnetisation component of low to medium coercivity.

Step	NRM (mA/m)	D (°)	I (°)
NRM	14 05	342 0	74 2
5 mT	12 06	358 4	71 0
10 mT	7 90	359 7	69 6
15 mT	5 16	4 0	69 6
20 mT	3 40	3 3	68 9
25 mT	2 20	10 2	69 0
30 mT	1 51	11 8	68 7
40 mT	0 87	23 3	68 6
50 mT	0 58	27 3	67 7

Table 39 Step-wise AF demagnetisation of specimen SC54 from section A D = declination (not variation corrected), I = inclusiveness of the NRM

Step	NRM (mA/m)	D (°)	I (°)
NRM	16 95	352 8	72 2
5 mT	13 69	6 4	68 7
10 mT	8 01	3 1	66 9
15 mT	4 89	8 3	67 3
20 mT	3 05	8 1	66 5
25 mT	1 87	8 4	67 3
30 mT	1 28	12 1	66 2
40 mT	0 68	52 2	67 2
50 mT	0 53	17 8	66 9

Table 40 Step-wise AF demagnetisation of specimen SC74 from section B

A4 2 13 The ChRM directions of most specimens were stable, with median destruction fields (MDF) of the NRM between 10mT and 13mT (Fig 74). Only two specimens (one from each section) failed to produce a reliable ChRM direction. Less than 5% of the NRM survived by 50mT demagnetisation, suggesting no significant contribution of antiferromagnetic minerals, like haematite and goethite, to the natural remanence. This, combined with the low MDFs, again points to (titano) magnetites and/or maghemites as the main carriers of NRM, and not to iron sulphides. The ChRM direction of each specimen was calculated using principal component analysis based on the 'least-squares fitting technique' of Kent *et al* (1983), on the basis of the three to four demagnetisation steps. Figure 75 shows the main magnetic parameters combined with the curves of declination and inclusiveness of the specimens' ChRM components (Table 38).

A4 2 14 The specimens from sections A and B exhibit similar ChRM declinations, whilst the ChRM inclusivenesses are a little steeper in section B than those in section A (Fig 75). We find no solid evidence for systematic secular variation trends, in the declination and inclusiveness data, that might indicate the sediment fill was deposited over an extended period of time. Hence, averaging of the directions for each of the sections is likely to be the most suitable dating procedure.

A4 2 15 The mean specimen-based archaeomagnetic directions from sections A and B are

section A (fills 12099, 12098, 12097)

$D = 25^\circ, I = 69.3^\circ$ ($\alpha_{95} = 2.2^\circ, K = 401, N = 12$),

section B (fills 12096, 12095)

$D = 357.9^\circ, I = 69.9^\circ$ ($\alpha_{95} = 1.9^\circ, K = 497, N = 12$)

A4 2 16 These mean archaeomagnetic directions need to be corrected for the magnetic declination at the site. The IGRF model predicts that the latter is 3.0° W for the site location (NASA 2006). The site was, however, situated immediately beneath the wires of a high-voltage line, so extra care was taken in determination of the magnetic variation at ground level. The magnetic declination at the site was determined (on 1st August 2006) using a sun compass. Four readings were taken with the sun compass (*ie* the azimuth of the sun shade was recorded on four occasions between 12.38 and 14.29 on that day). They produced estimates of the local magnetic north of $1.7^\circ, 2.6^\circ, 1.8^\circ$, and 2.4° . Their mean is 2.1° E. The latter estimate of the local declination was used in the following analysis.

A4 2 17 The variation-corrected archaeomagnetic directions for the Scots Dyke sections are

section A (fills 12099, 12098, 12097)

$D = 4.6^\circ, I = 69.3^\circ$ ($\alpha_{95} = 2.2^\circ, K = 401, N = 12$),

section B (fills 12096, 12095)

$D = 0.0^\circ, I = 69.9^\circ$ ($\alpha_{95} = 1.9^\circ, K = 497, N = 12$)

A4.3 ARCHAEOMAGNETIC DATING OF THE SECTIONS

A4 3 1 The mean directional results were converted via the pole method of Noel and Batt (1990) in order to compare it to the revised British master curve of Clark *et al* (1988). This corrects the direction to Meriden ($\phi = 52.43^\circ$ N, $\lambda = 1.62^\circ$ W) (Fig 76). Converted to Meriden data

section A (fills 12099, 12098, 12097)

$D = 4.5^\circ, I = 68.1^\circ$ ($\alpha_{95} = 2.2^\circ, K = 401, N = 12$),

section B (fills 12096, 12095)

$D = 0.0^\circ, I = 68.8^\circ$ ($\alpha_{95} = 1.9^\circ, K = 497, N = 12$)

A4 3 2 When plotted on the UK master curve of Clark *et al* (1988), the mean direction for section A (fills 12099, 12098, 12097) gives a best estimate age for the sediment fill of AD 70, with an approximate 95% confidence interval of AD 30-110. There are two possible solutions for the age of the sediment fill in the lower section B: 90-70 BC, or AD 1-110, with an approximate 95% confidence interval. The most likely date in the second case is AD 40. This means that the sediment fill in both sections A and B probably formed in quick succession during the first century AD, during the interval of about

AD 40-70 (95% confidence date range AD 1-110), indicating ditch construction some time during or prior to the early part of the first century AD

A4.4 ARCHAEOMAGNETIC DATING SUMMARY

A4.4.1 Table 41 summarises the dating for sections A and B

Archaeomagnetic ID	SC (section A)
Feature	upper sedimentary section, contexts 12099, 12098, 12097
Location	Longitude 359.2994°E , Latitude 54 0453°N
Number of Samples (taken/used in mean)	13/12
AF Demagnetisation Applied	9-23mT (line-fit range)
Distortion Correction Applied	0 0°
Declination (at Meriden)	4.5°
Inclination (at Meriden)	68 1°
Alpha-95	2 2°
k	401
Date range (63% confidence)	AD 70 to AD 75
Archaeomagnetic ID	SC (section B)
Feature	lower sedimentary section, contexts 12096, 12095
Location	Longitude 359.2994°E , Latitude 54 0453°N
Number of Samples (taken/used in mean)	13/12
AF Demagnetisation Applied	9-23mT (line-fit range)
Distortion Correction Applied	0.0°
Declination (at Meriden)	0.0°
Inclination (at Meriden)	68 8°
Alpha-95	1 0°
k	497
Date range (63% confidence)	AD 30 to AD 80

Table 41 Summary of archaeomagnetic dates for the ditch fills in the Scots Dyke

A4.5 BACKGROUND TO ARCHAEOMAGNETISM AND ARCHAEOMAGNETIC TECHNIQUES

A4.5.1 *The Earth's magnetic field:* the magnetic field of the Earth is generated within the core, due to a magnetodynamo effect. The form of this magnetic field at the Earth's surface is such that it can be ascribed to a two-component system. The first, the dipole component, is the main component of the magnetic field. This can be equated to a bar magnet with a fixed north and south pole, which are effectively located over the Geographic North and South Pole respectively. The inclination of this dipole field is systematically related to the latitude of observation by $\tan(I) = 2 \tan(\lambda)$ ($I =$

inclination, λ = latitude) This relationship is such that near the present-day North Pole the magnetic field is steeply dipping downwards, and near the equator, the field is shallowly dipping and directed northwards

A4 5 2 The second element of the magnetic field, which is most important for archaeomagnetic studies, is the non-dipole component This is a subsidiary magnetic field that can be described by a complex set of Fourier harmonics This non-dipole field varies in intensity and direction through time (the change is called *secular variation*) and gives rise to the current displacement of the magnetic pole into the region of Arctic Canada If the magnetic field direction is fossilised in archaeological contexts (like during short heating events in hearths, ovens and kilns), the recorded direction will match the direction of this secular field

A4 5 3 *Types of magnetic minerals:* there are several types of minerals that can act as recorders of the magnetic field (Table 42) Each of these minerals can retain a remanent magnetisation Magnetite and its magnetically similar titanomagnetite-group minerals (eg Fe_3O_4 to Fe_2TiO_4 solid solution) are often the most important, because these are strongly magnetic and abundant and are very common in all kinds of archaeological materials

Mineral group	Composition	Typical origin	Magnetic characteristic	Curie temperature
Magnetite	Fe_3O_4	Detrital/soil/heating-generated	Low coercivity	580 °C
Haematite	Fe_2O_3	Detrital/ weathering	High coercivity	710 °C
Greigite	Fe_3S_4	Anoxic ditch fills, and features	Moderate coercivity	~320 °C
Goethite	αFeOOH	Weathering	Very high coercivity	~120 °C

Table 42 The main groups of magnetic minerals that are significant in carrying remanent magnetisation, and some of their properties

A4 5 4 Within each mineral group, a number of factors influence the magnetic properties of these minerals These various properties can be useful in a) distinguishing which mineral is carrying the remanent magnetisation, and b) allowing the separation and isolation, during demagnetisation, of the recorded magnetic field information carried by different minerals

A4 5 5 *Temperature* each magnetic mineral has a specific upper temperature, above which it can no longer retain its remanent magnetisation This temperature is its *Curie temperature*, and can be diagnostic of the mineral carrying the remanence

A4 5 6 *Grain size* the size of the magnetic particle is a fundamental control on its magnetic behaviour This is primarily expressed through the grain's *coercivity*, which can be thought of as the degree of difficulty with which the direction of the intrinsic remanent magnetisation can be reset without physically rotating the grain Generally, within any mineral group, the larger the grain size, the smaller the coercivity (ie more easily reset) Unfortunately, grain-size - coercivity relationships are not quite as simple as this, and it is often best to talk about *multidomain* (largest grains) and *single-domain*

grams (mostly smallest grains), when describing magnetic grain behaviour Single-domain grains are the most resistant to resetting, and carry the most important archaeomagnetic information, so it is the direction of the magnetic field recorded by these grains that demagnetisation is trying to isolate

A4 5 7 In addition to differences in grain size controlling coercivity, different minerals can have markedly different coercivity. For example, magnetite and magnetic sulphides (eg greigite) have a relatively low coercivity, compared to haematite, the coercivity of which is approximately one order of magnitude larger than magnetite of the same grain size

A4 5 8 **Introduction to demagnetisation procedures** the remanent magnetisation of any specimen, once it has been collected and first measured, is called the Natural Remanent Magnetisation (NRM). This NRM may be composed of several components, namely the Characteristic Remanent Magnetisation component (ChRM), acquired at (or close to) the time of last heating (or deposition for a sediment), and any later *overprints* which may have been acquired after this time. It is the purpose of demagnetisation to remove these overprints, so the ChRM direction can be defined

A4 5 9 There are various methods of demagnetising rocks, the two most commonly used being alternating field (AF) methods and thermal methods (Table 43)

Method	Equipment used	Procedure	Minerals effective on	Treatment range
Alternating Field Demagnetisation (AF)	Alternating magnetic field applied to specimen in zero direct field	AF ramped to peak field, and slowly reduced	Magnetites, Magnetic sulphides	0-100mT peak AF fields
Thermal Demagnetisation	Specimen oven inside a zero magnetic field	Specimen heated to peak temperature for ~20 minutes, and cooled in zero magnetic field	Magnetite, Haematite, Magnetic sulphides, Goethite	50-720 °C

Table 43 Main types of demagnetisation methods and their characteristics

A4 5 10 **Alternating Field (AF) Demagnetisation** the specimen is randomly tumbled in an alternating magnetic field, which is slowly reduced in intensity from a peak value to zero (the specimen and alternating field are inside a magnetic shield which reduces the ambient Earth's magnetic field to near zero). This procedure randomises the magnetic moments of grains with coercivities up to the value of the applied field. Progressively larger peak fields are applied to remove magnetic components due to grains with larger coercivities. Typically, AF magnetic fields in increments of 5mT, or 10mT, are used. Between each demagnetisation step, the remanent magnetisation of the specimen is measured, which allows analysis of the behaviour of the NRM as it is slowly stripped away

A4 5 11 **Thermal Demagnetisation** specimens are heated to a specific temperature and then allowed to cool to room temperature in a zero magnetic field. Heating a specimen in this way randomises the magnetisation of specific types of magnetic grains. The grains that are randomised at this temperature are those whose 'blocking temperature' is less than this temperature. Thermal

demagnetisation is thought to be particularly effective in isolating magnetisation due to thermo-viscous or thermo-remanent causes (*eg* caused by heating in a fire/hearth *etc*) It is also the only way to demagnetise remanence carried by haematite or goethite, because routine AF demagnetisation equipment cannot achieve large enough magnetic fields to exceed the coercivity of remanence of these minerals

A4.6 PRESENTATION OF DEMAGNETISATION DATA

A4 6 1 Demagnetisation data for specimens is displayed in three ways, using diagrams like Figure 74. Graphs in these demagnetisation figures are composed of a) Zijderveld diagram, b) stereographic projection, and c) a J/J_0 plot (intensity decay plot). These graphs display the specimen demagnetisation data rotated into the *in situ* (field) orientation.

A4 6 2 *The Zijderveld diagram* this presents both the directional and magnitude information of the remanence vector as it is demagnetised. In these diagrams, the distance from the origin (crossing point of axes) corresponds to the magnitude of the remanence vector. Equal intensity scale between axis ticks is used on each of the four axes, and is shown on the diagram in mA/m (Fig 74). As a result of demagnetisation, the NRM vector generally plots furthest from the origin, and the last demagnetisation step nearest the origin.

A4 6 3 The remanence vector directional information, which is three-dimensional, is reduced to the two-dimensions of the paper by projecting the position of the vector onto two orthogonal planes, a horizontal one and a vertical one (indicated on the diagram with filled and open symbols). An axis common to both projection planes is shared in the diagram (*eg* E, up, W, down). The vertical projection planes are either east/west or north/south, depending upon which projection is suitably oriented for displaying the maximum spread in data points. The vertical plane in Figure 74 is aligned north/south.

A4 6 4 The most important point to appreciate is that the removal of a single component of magnetisation results in straight lines (one for each projection) on the Zijderveld diagram, connecting demagnetisation steps. Specimens which have curved segments on Zijderveld diagrams do so because the coercivity spectra (or blocking temperature spectra) of the ChRM and other magnetisations overlap.

A4 6 5 *Stereographic Projection* the direction of the remanence vector is plotted on an equal area stereographic projection, which displays only the directional information, with negative inclusion (i.e. anomalous in archaeological context) plotted as open circles and positive inclusions (potentially of archaeological significance) with filled circles. The horizontal projection plane of the Zijderveld diagram is comparable to the stereographic projection.

A4 6 6 *J/J_0 plot* this displays the remanence intensity decay with either the AF demagnetisation field, or temperature. The intensity is normalised to the initial NRM intensity (i.e. NRM intensity = 1.0), and the NRM intensity (J_0) in mA/m (10^{-3} A/m) is shown just above the diagram. The intensity will

generally decay, the larger the demagnetisation value used, the shape of this decay can be diagnostic of the stability of the remanence

A4.7 GLOSSARY OF ARCHAEOMAGNETIC TERMS

- A4 7 1 **α_{95} (*Alpha 95*)** this is a measure of angular dispersion (in degrees), commonly used in directional statistics, which is derived from *Fisher Statistics*. It is the angular radius of a cone about the mean direction, in which the true population mean is found. There is 95% probability that the population mean lies within this range, about the mean direction (*ie* five pure chances in a 100 that the true mean direction lies outside the confidence cone)
- A4 7 2 ***Blocking temperature*** this is the transition temperature between when a grain is superparamagnetic and single domain. In essence, for each magnetic particle there is a specific temperature (below the Curie temperature), above which it can no longer retain its remanent magnetisation - *ie* its blocking temperature. The blocking temperature is strongly grain-size dependent, with very small *single domain* particles having lower blocking temperatures than slightly larger single domain grains
- A4 7 3 ***Coercivity (or coercive force)*** this is the ease with which the remanent magnetisation of a grain or specimen can be reset into a new direction (*ie* magnetised, or demagnetised, in this direction) by an applied magnetic field. This is measured in terms of the magnetic field (in MilliTesla, mT) required to do this. The coercivity of a mineral is strongly related to its grain size, such that smaller grains (above the superparamagnetic size threshold) need a larger magnetic field than bigger grains in order to 'demagnetise' them
- A4 7 4 ***Coercivity spectra*** a specimen's remanent magnetic properties are due to a mineral (perhaps two or more minerals), of various grain sizes. Consequently, the magnetic field (coercive force) required to 'demagnetise' these variously sized magnetic particles will also vary over a range of values. This can be quantified by the Median Destructive field - that coercivity at which 50% of the NRM has been destroyed
- A4 7 5 ***ChRM (Characteristic Remanent Magnetisation)*** this term is used to describe what is believed to be a specimen's remanent magnetisation, produced when the material was formed or last heated. The ChRM is generally (but not always) interpreted to be the last component (*ie* linear segment going through the origin of the Zijderveld plot) recoverable from the demagnetisation data
- A4 7 6 ***Declination*** the angle between north and the horizontal projection of the magnetisation vector, *ie* 0° = North directed, 180° = South directed, 90° = East directed, 270° = West directed. In specimens from unoriented core material, the declination is measured from the specimen fiducial direction

- A4 7 7 **Ferrimagnetic/Ferromagnetic** these are minerals which can acquire a permanent magnetisation, that can be retained in the absence of an applied magnetic field (eg magnetite) There are several sub-groups of magnetic behaviour within this broad grouping These minerals generally have a large magnetic susceptibility compared to paramagnetic and diamagnetic materials Common examples are titanomagnetites, haematite (canted antiferromagnetic), pyrrhotite/greigite (ferrimagnetic)
- A4 7 8 **Fisher statistics** this is the commonly used statistical method of averaging three-dimensional vectors (Butler 1992), the 3-D equivalent of the one-dimensional normal statistics
- A4 7 9 **Inclination** this is the angle between horizontal and the magnetisation vector, such that a downwards-directed vector has positive inclination, and an upwards-directed vector has negative inclination
- A4 7 10 **Induced magnetisation** see Magnetic susceptibility and Magnetisation (Sections A4 7 12 and A4 7 13)
- A4 7 11 **Koenigsberger factor (Q_{NRM})** this is the ratio of the induced (determined from the magnetic susceptibility) and remanent magnetisation (determined from the NRM intensity) Values larger than one indicate the net magnetisation is more than 50% dominated by the remanence Materials that have been significantly heated often have large values of Q_{NRM} , hence it is often used as an indication of the nature and 'stability' of the remanent magnetisation
- A4 7 12 **Magnetic susceptibility** when a material is exposed to a magnetic field (H), it acquires an *induced magnetisation*, J_i , such that $J_i = \chi H$, where χ is the magnetic susceptibility All materials possess a magnetic susceptibility, including *diamagnetic*, *paramagnetic* and *ferrimagnetic* materials, but because ferrimagnetic materials (eg magnetite) have magnetic susceptibility several orders of magnitude larger than paramagnetic materials, it is common to think of magnetic susceptibility as a measure of the 'concentration of magnetic materials' Volume-specific magnetic susceptibility has no units in SI (ie J_i and H have same units), but when expressed on a mass specific basis, its units are $m^3 Kg^{-1}$
- A4 7 13 **Magnetisation** the magnetisation of a material is the net magnetic moment per unit volume There are two types of magnetisation, *induced* and *remanent magnetisation* The *induced magnetisation* is associated with the magnetic susceptibility, and is ONLY found and measured when materials are in a weak magnetic field Remanent magnetisation is a 'permanent magnetisation' and is that which enables rocks to record the direction of magnetic fields at their time of formation
- A4 7 14 **Median Destructive Field** see Coercivity spectra (Section A4 7 4)
- A4 7 15 **Multidomain** see Single domain (Section A4 7 20)

- A4 7 16 **NRM** (**Natural Remanent Magnetisation**) this is the remanent magnetisation of a rock, as it is first measured, prior to laboratory treatment. This may be composed of one or more magnetisation components, perhaps acquired in different times and under different processes.
- A4 7 17 **Paramagnetic** minerals that acquire an induced magnetisation in the direction of an applied magnetic field are paramagnetic. These also have a positive magnetic susceptibility, generally related to the Fe- and Mn-content of the phase. When the magnetic field is removed, they retain NO remanent magnetisation. Common examples of these are Fe- or Mn-bearing silicates and carbonates.
- A4 7 18 **PTRM** when material is heated, and subsequently cooled in a magnetic field below the Curie temperature of the magnetic minerals responsible for remanence, the material will acquire a partial thermoremanent magnetisation, in the direction of the magnetic field. This is due to the fact that minerals, as a result of their varying grain size (and other factors), have a range of blocking temperatures.
- A4 7 19 **Remanent magnetisation** this is the magnetisation of a specimen which is permanent, and can be likened to that of a bar magnet, having a north and a south pole (*ie* it has vector properties). The remanent magnetisation vector is expressed in terms of *declination*, *inclination* and magnitude. When this magnitude is expressed on a volume-specific basis, its units are A/m (or mA/m = 10^{-3} A/m), but on a mass-specific basis (to allow for changes in density), its units are $\text{Am}^2 \text{Kg}^{-1}$ (magnetic moment per Kg).
- A4 7 20 **Single domain** in ferromagnetic particles, as a result of the energy-charge configuration, individual magnetic particles may be internally sub-divided into *domains*. These domains each have a different directional alignment of the magnetisation, and contribute to the overall magnetisation of the whole grain. When the particles are small ($< \sim 0.1 \mu\text{m}$ for spherical magnetite), these particles consist of only one domain, and are called *single domain* grains. When magnetite particles are larger than $10 \mu\text{m}$, they consist of lots of domains. This type of particle is called a *multidomain* grain. Single domain and multidomain grains of a specific mineral each have characteristic magnetic properties. Unfortunately, natural magnetic particles also come in different shapes, and are intergrown or sub-divided by other (perhaps non-magnetic) sub-regions, so that 'magnetic grain size' (*ie* single domain or multidomain behaviour) may not correspond to the physical size of a magnetic grain. For example, a magnetite particle of say $30 \mu\text{m}$ may be sub-divided internally so that this single grain may possess single domain *and* multidomain behaviour, or perhaps only single domain behaviour.
- A4 7 21 **Susceptibility** see Magnetic susceptibility (*Section A4 7 12*)
- A4 7 22 **Superparamagnetic** particles which display ferromagnetic/ferrimagnetic behaviour can also be superparamagnetic when these grains are very small. This means that they can retain a remanent magnetisation, but only for a very short period of time. The time over which this retention occurs is grain size-dependent (superparamagnetic magnetite grains are $< \sim 0.02 \mu\text{m}$), perhaps

from 10^{-10} s to a convenient value of 100s considered by Butler (1992) Such superparamagnetic grains lose the retained remanence due to thermal agitation of the atoms In many ways, such grains are similar to paramagnetic grains, and do not carry a palaeomagnetic remanence

A4 7 23 **Thermo-Remanent Magnetisation (TRM)** this is the magnetisation acquired when the grain cools through its Curie temperature

A4 7 24 **VRM (Viscous Remanent Magnetisation)** this is remanent magnetisation which is acquired by magnetic grains when exposed to a weak magnetic field over a period of time This may 'overprint' the original magnetisation of the material acquired at the time of formation The magnitude of VRM acquisition can be described by $S \log(t)$, where S = the viscosity coefficient and t is time S is related to the grain volume, whether it is a multidomain or single domain grain, and the temperature (Butler 1992) Generally, multidomain grains acquire VRM much faster than single domain grains

A4 7 25 **Zijderveld diagram** this is a standard method of displaying the remanent magnetisation of a specimen as it is progressively demagnetised (also called vector end point, vector component, or orthogonal projection diagrams) The use of Zijderveld diagrams in interpreting the demagnetisation behaviour of specimens is important for reliable studies This is because such diagrams allow the user to evaluate when a magnetic component is being removed, and if it may overlap with another magnetic component in the specimen

APPENDIX 5 OPTICALLY STIMULATED LUMINESCENCE DATING

A5.1 TECHNICAL SUMMARY

A5 1 I Samples of sediment from three sediments (fills 12095, 12097, 12099) within the Scots Dyke ditch (12035) at SCA10 were taken for optically stimulated luminescence (OSL) dating on 18th July 2006 (PI 63), by members of the Luminescence Dating Laboratory, guided by site staff from OA North. The laboratory references for these samples are given in Table 44.

Lab Reference	Context	Site Reference	Luminescence date ⁽¹⁾
Dur06OSLQ1 330-1	12095	OA North sample 250	AD 65 ±150, ±240
Dur06OSLQ1 330-2	12097	OA North sample 251	120 BC ±70, ±220
Dur06OSLQ1 330-3	12099	OA North sample 252	AD 510 ±90, ±135

(1) The uncertainties associated with each date are given at the 68% level of confidence, since the application of the Student's t test indicated that the dates for 330-1 and 330-2 were not distinguishable at the 95% level of confidence. The first error is used when comparing luminescence ages from the same laboratory and the second error term should be used when comparing luminescence dates with independent dating evidence.

Table 44 Results of OSL dating of selected sediments within the Scots Dyke ditch (12035) at SCA10

A5 1 2 The samples were prepared by sub-sampling the inner volume of the cores under subdued red lighting in the laboratory, quartz in the grain size range 90-150 µm was subsequently extracted from the sediment using standard procedures for the inclusive fusion technique (Aitken 1985). The results of initial suitability tests with all samples indicated that all three samples were potentially suitable for OSL dating.

A5 1 3 An OSL technique based on a single aliquot regenerative dose (SAR) procedure (Murray and Wintle 2000, 2003) was used to determine the absorbed dose accumulated since the last exposure of the sediment to daylight (the palaeodose, P). Measurements were made using a Risø TL-DA-12 automated reader, and laboratory doses were administered by a calibrated ⁹⁰Sr/⁹⁰Y beta source mounted on the reader. OSL was observed under stimulation by light from blue LEDs and the luminescence was detected in the ultraviolet region using an EMI photomultiplier, in combination with a Hoya U340 optical filter.

A5 1 4 The distribution of values of P (one value per aliquot tested) for all samples indicated more uniform pre-depositional exposure to daylight in the case of samples 330-2 and 330-3, compared with the basal sample, 330-1. However, this does not preclude the occurrence of incomplete zeroing of the stored charge before burial in all three samples.

A5 1 5 The average total annual dose, D_T , was derived from a combination of experimental techniques and calculation. The beta dose-rate within the sampled sediment medium, using the β TLD technique (Aitken 1985, Bailiff 1982) and the gamma dose-rate, were calculated using the concentrations of ^{238}U , ^{232}Th and ^{40}K , determined using a high-resolution Ge gamma spectrometer, readings obtained using a portable NaI detector on site were also used in the assessment of the gamma dose-rate. Adjustment of the beta and gamma dose-rates to account for the uptake of moisture in the sample medium was based on the assumption that the average water uptake in the sample medium during burial was $\times 0.8 \pm 0.2$ (samples 330-2, 330-3) and $\times 1.0 \pm 0.2$ (sample 330-1) of the value measured in the laboratory. It was assumed that the measured radionuclide and water content of the sediments was typical of the surrounding matrix. The contribution to the annual dose due to cosmic rays was estimated using data published by Prescott and Hutton (1988).

A5 1 6 The luminescence age was calculated using the age equation below (Table 45). The uncertainty in the age was calculated by taking into account the propagation of errors associated with experimental measurements, and takes into account those errors associated with the calibration and conversion factors (Aitken 1985).

$$\text{Luminescence Age (years)} = \frac{\text{Palaeodose (mGy)}}{\text{Annual dose (mGy/year)}}$$

Palaeodose (mGy)	Annual dose (mGy/a)	Annual dose components (%)		Water (%)
		β	γ +cosmic	
5270 \pm 400	2.89 \pm 0.06	58	42	37 \pm 7
5500 \pm 140	2.59 \pm 0.05	57	43	37 \pm 7
3210 \pm 150	2.15 \pm 0.08	49	51	23 \pm 5

Table 45 Values used to calculate luminescence age

A5 1 7 After subtraction of the test year (2006) from the luminescence age, the luminescence date is given with two associated errors at the 68% level of confidence, based on the specification by Aitken (1985).

$$\text{Luminescence Date} \pm \sigma_A, \pm \sigma_B$$

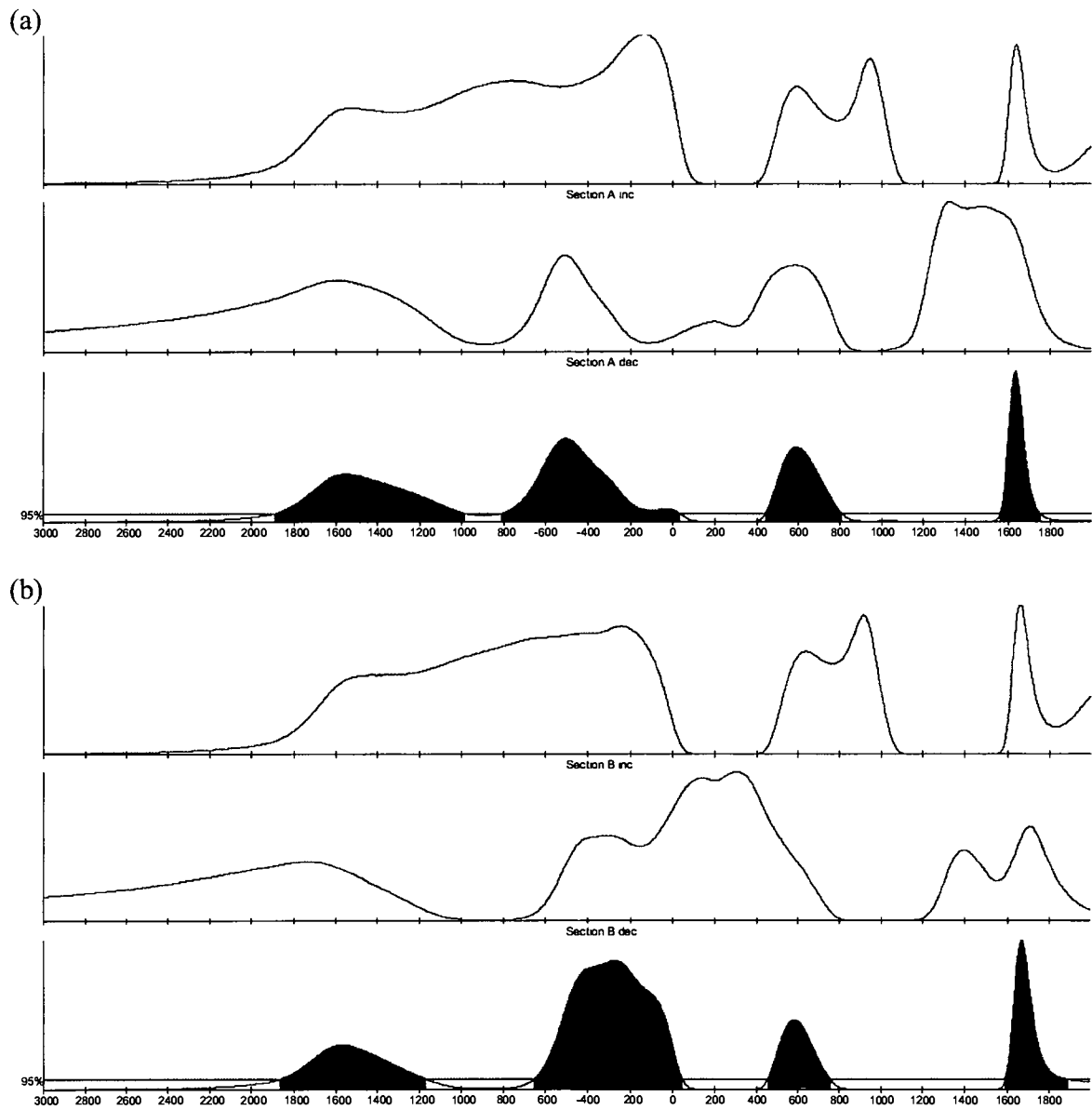
The first error term, σ_A , is a type A standard uncertainty obtained by an analysis of repeated observations (*ie* random error) and should be used when comparing results with other luminescence dates from the same laboratory. The second error term, σ_B , is a type B standard uncertainty, based on an assessment of uncertainty, associated with all the quantities employed in the calculation of the age, including those of type A (*ie* random and systematic errors). The second error, σ_B , should be used when comparing luminescence dates with independent dating evidence. This method of error assessment is derived from an analysis of the propagation of errors and, providing the distribution of errors is normal, the approach appears to be sufficiently

robust The calculations assume that the zeroing of the luminescence before the last burial was fully effective

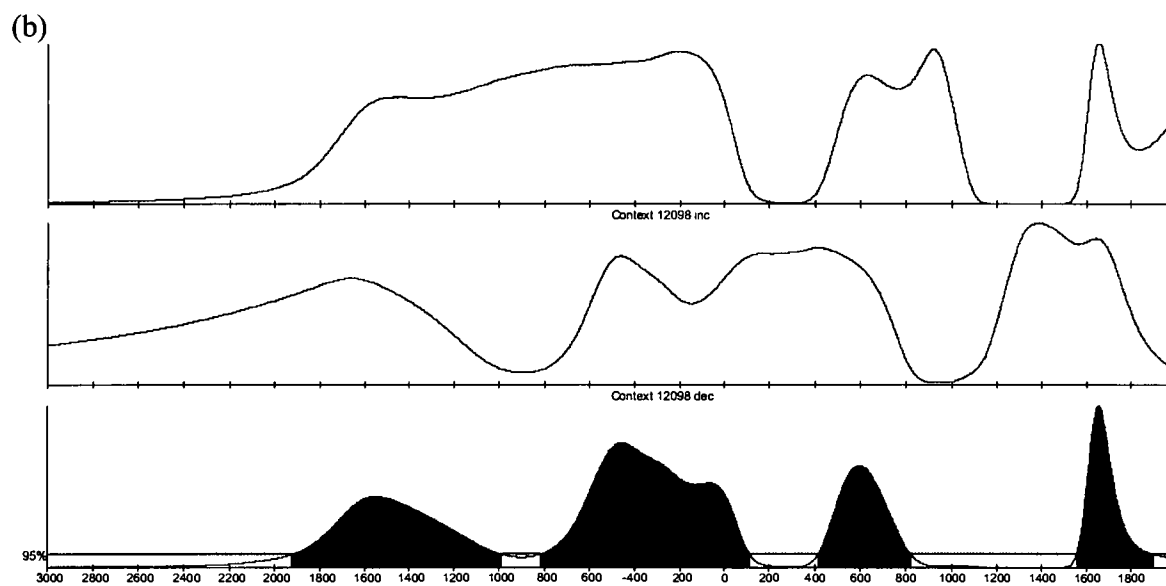
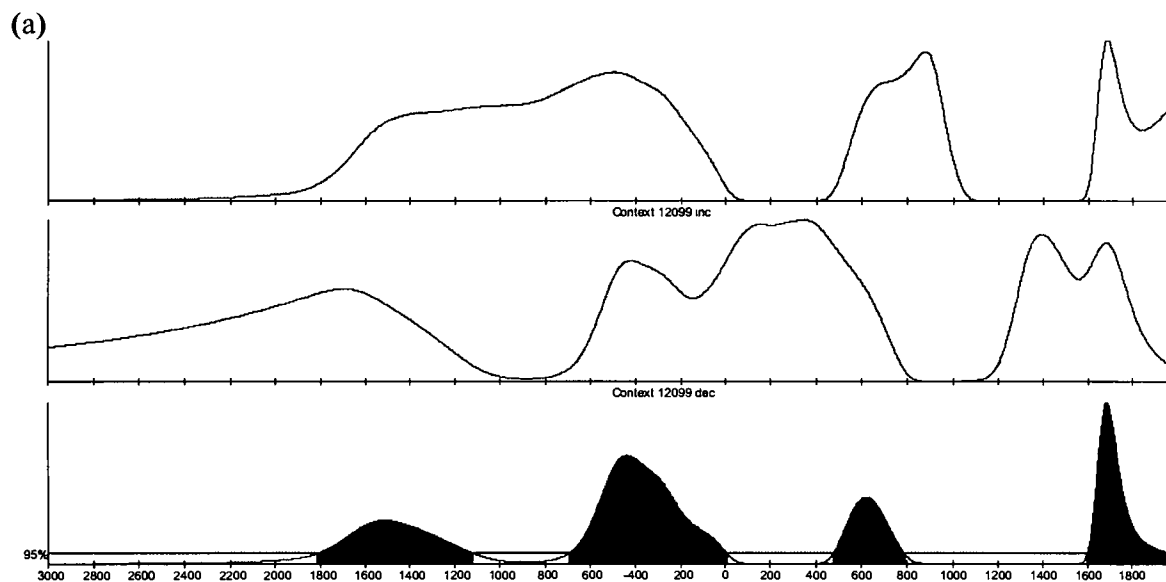
A5 1 8 Fluctuation in moisture content of sediments during burial is a dominant source of uncertainty when dating sediments from sites in temperate climates. The change in luminescence date with average moisture content (expressed as a percentage of dry sample weight) during burial (Fig 77) illustrates this dependency. The arrow indicates the value of the sample moisture content measured in the laboratory

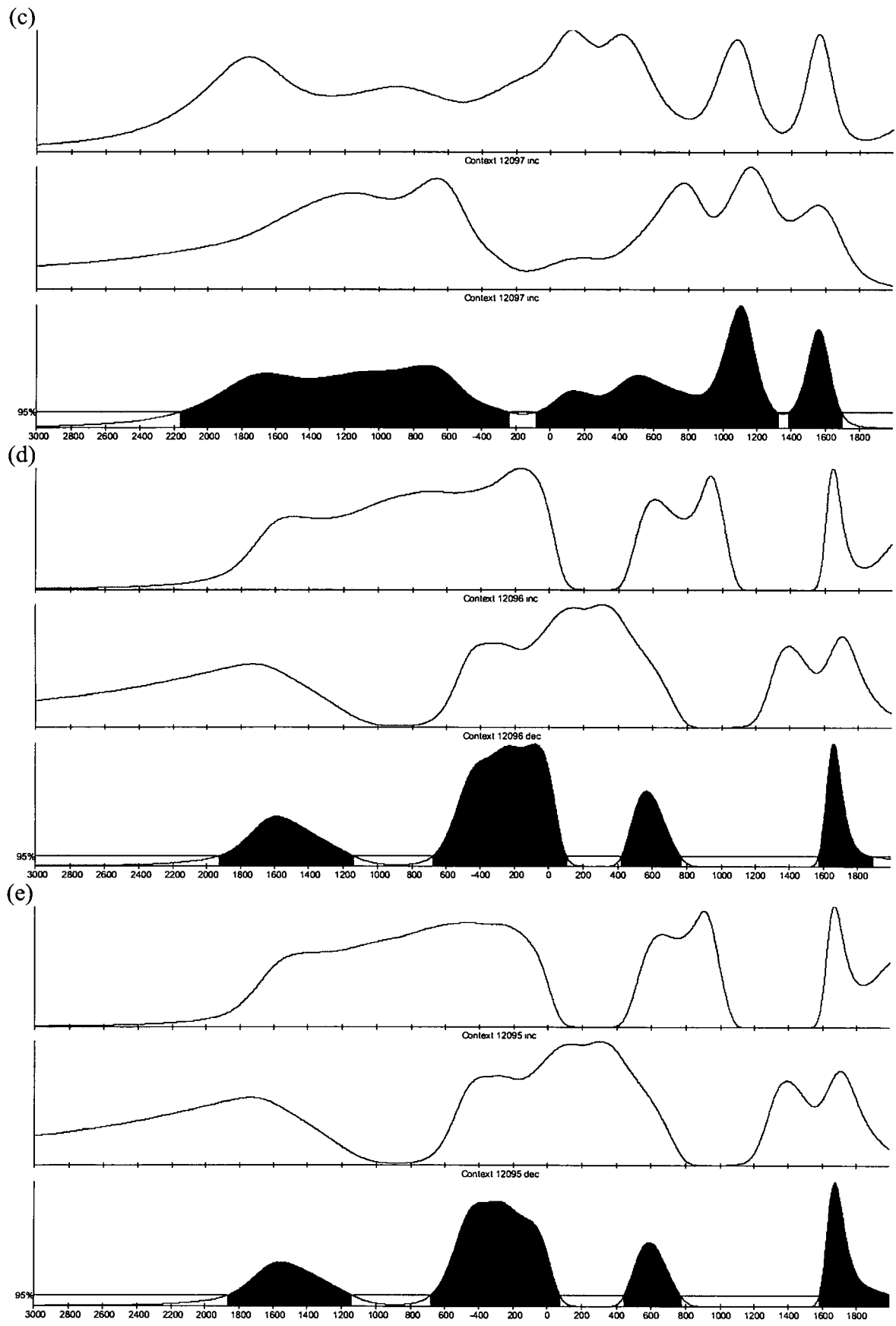
APPENDIX 6 INTEGRATED DATING ANALYSIS ADDITIONAL FIGURES AND TABLES

A6.1 PROBABILITY DISTRIBUTIONS OF ARCHAEOMAGNETIC DATES FOR (A) SECTION A AND (B) SECTION B, GENERATED WITH RENDATE



A6.2 PROBABILITY DISTRIBUTIONS OF ARCHAEOMAGNETIC DATES FOR (A) FILL 12099, (B) 12098, (C) FILL 12097, (D) FILL 12096, (E) FILL 12095, GENERATED WITH RENDATE





A6.3 DETAILS OF RADIOCARBON DATES FOR THE THREE MODELS

Name	Modelled (BC/AD)			Agreement (%)	Convergence (%)
	from	to	%		
Sequence Dyke				$A_{\text{model}}=98.1$ $A_{\text{overall}}=100.6$	
Boundary Start	-1711 -1676	-1682 9	0.2 95.2		96.9
Phase section B					
Prior ArchaeomagB	-561	41	95.4	127	99.4
C_Date 330-1	-471	222	95.4	95.9	99.9
Phase section A					
Sequence OSL					
C_Date 330-2	-240	396	95.4	88.8	99.9
C_Date 330-3	217	740	95.4	101.3	99.9
Prior ArchaeomagA	-280 420 1597	76 799 1670	16.4 76.7 2.2	92.5	98.9
Boundary End	197 222	214 2002	0.1 95.3		97.9

Table 46 Full OxCal results for the Two Section model

Name	Modelled (BC/AD)			Agreement (%)	Convergence (%)
	from	to	%		
Sequence Dyke				$A_{\text{model}}=82.5$ $A_{\text{overall}}=84.1$	
Boundary Start	-1116	-45	95.4		96.6
Phase 12095					
Prior Archaeomag 12095	-557	20	95.4	134.9	99.9
C_Date 330-1	-480	48	95.4	81.2	99.9
Prior Archaeomag 12096	-335	105	95.4	134.9	99.9
Phase 12097					
Prior Archaeomag 12097	-194	556	95.4	66.7	99.9
C_Date 330-2	-212	437	95.4	91.3	99.8
Prior Archaeomag 12098	-55	645	95.4	85.4	99.9
Phase 12099					
Prior Archaeomag 12099	451	787	95.4	78.1	99.9
C_Date 330-3	332	773	95.4	102.4	99.9
Boundary End	528	1592	95.4		97.7

Table 47 Full OxCal results for the Context model

Name	Modelled (BC/AD)			Agreement (%) $A_{\text{model}}=60.9$ $A_{\text{overall}}=65.6$	Convergence (%)
	from	to	%		
Sequence Dyke					
Boundary Start	-970	-105	95.4		96.5
Phase 12095					
Prior Archaeomag 12095	-525	-41	95.4	140.4	99.8
C_Date 330-1	-356	-24	95.4	48.8	99.8
Prior Archaeomag 12096	-268	19	95.4	151.1	99.9
Phase 12097					
Prior Archaeomag 12097	-162	523	95.4	61.9	99.7
C_Date 330-2	-177	68	95.4	79.7	99.8
Prior Archaeomag 12098	-60	614	95.4	77.7	99.7
Phase 12099					
Prior Archaeomag 12099	435	762	95.4	76.4	99.8
C_Date 330-3	376	697	95.4	100.1	99.8
Boundary End	522	1325	95.4		96.3

Table 48 Full OxCal results for the Context model, using only random errors on OSL dates (the Third Model)

APPENDIX 7 SURVEY OF HISTORIC STREET FURNITURE AND FIELD WALLS

A7.1 INTRODUCTION

A7.1.1 This report outlines the results of a survey of historical street furniture and field walls along the route of the A66 improvements from Greta Bridge to Scotch Corner, to satisfy *Section 11.1.10* of the *Employer's Requirements* (HA 2005), which states that

'Based on the review of the available data, and guided by the Outline Archaeological Design Brief in Annex 11/1, the Contractor's Archaeologist shall identify the need for additional surveys. These surveys should also include for a survey of field walls and street furniture likely to be affected by the scheme

Further details on the requirement for undertaking the field wall survey can be found in *Section 13* of the *Employer's Requirements Annex 11/1* (HA 2005), paragraphs 3.2.15 and 3.3.21

A7.1.2 The aims of the survey were to

- identify any historical street furniture, agricultural miscellany or field walls that would be affected by the scheme,
- make a record of the location, form and condition/state of preservation of the features,
- make recommendations for further detailed and measured recording that may be deemed necessary to ensure the preservation by record of important features, and
- make recommendations for the retention, relocation or reconstruction of features of historic/aesthetic importance

A7.2 METHODOLOGY

A7.2.1 To ascertain the presence of historical street furniture, agricultural miscellany or field walls that would be affected by the scheme, a desk-based assessment was undertaken. This assessment comprised a review of the following sources

- Highways Agency (HA) 2002a *A66 Greta Bridge to Stephen Bank Environmental Statement Volume 2 – Part 3 Cultural Heritage*,
- Highways Agency (HA) 2002b *A66 Carkin Moor to Scotch Corner Environmental Statement Volume 2 – Part 3 Cultural Heritage*,
- Northern Archaeological Associates (NAA) 1997 *A66 Upgrading to Dual Carriageway Area A Scotch Corner to Greta Bridge Stage 2 Archaeological Assessment*, NAA 97/16, unpublished report,
- North Yorkshire Historic Environment Record,

- Co Durham Historic Environment Record,
- Keys to the past*, Durham County Council SMR Online
<http://www.keystothepast.info/k2p/usp.nsf/pws/keys+to+the+Past+-+home+page>
- English Heritage National Monuments Record (NMR) (which makes reference to milestone locations depicted on First Edition OS mapping),
- First Edition OS mapping (1857a, 1857b, 1857c)

A7 2 2 A site visit was undertaken in April 2006, whereby the locations of the features affected were recorded on plan, a basic description was made for each feature, and photographs were taken to record the form of the feature and to inform any potential future reconstruction or relocation works. Additionally, in advance of, and during, the preliminary clearance works on site, all those areas that would be affected by construction works were inspected to check for the presence of unrecorded items of historical street furniture.

A7 2 3 It should be noted that the full extents of the field walls that would be affected by the scheme were not photographed. It was considered sufficient to describe and photograph a selection of sections of field walls that were representative of the vast majority of the walls that would be affected.

A7.3 HISTORICAL STREET FURNITURE

A7 3 1 **Milestones:** the desk-based assessment identified the possible presence of four milestones that could be affected by the scheme. These comprised:

- Milestone on the south side of the A66, west of Rock Castle (NZ 1872 0680),
- Milestone on the south side of the A66, east of Blackhill Farm (NZ 1731 0761),
- Milestone on the north side of the A66, at the bottom of Stephen Bank (NZ 1290 1020),
- Milestone on the north side of the A66, 30m south-east of Thorpe Farm (NZ 1061 1182) Grade II Listed

A7 3 2 Only the existence of the listed milestone at Thorpe Farm was confirmed during the site survey. None of the other three milestones could be found, and it is therefore assumed that they had been removed. It was also confirmed that the listed milestone would not be affected by the proposed works, so no recording was undertaken.

A7 3 3 **Culverts:** the survey identified two locations along the length of the scheme where the existing A66 crossed culverted streams. The headwalls of these culverts, which are likely to be of mid-late twentieth-century date, were found to have been made of dressed stone topped with coping stones. The culverts are located as follows:

- Approximately 200m east of Carkm Moor Roman fort (NZ 1635 0819),
- Approximately 200m west of Smallways Inn (possibly known as New Smallways Bridge) (NZ 1117 1126)

A7 3 4 At the time of the survey, it was understood that the northern-facing headwalls of both culverts would need to be removed to facilitate the construction scheme. Therefore, further and more detailed measured recording of these headwalls was undertaken (*Section 4 5*)

A7 3 5 **Other features:** it was highlighted to the project team that a stone horse trough had been found at the junction of Warrener Lane and the A66, north of the carriageway (NZ 1649 0811). The trough was identified *in situ* and was subjected to a photographic survey (*Section 4 5 5*)

A7 3 6 A millstone was identified during topsoil stripping works at Black Plantation (approximate location NZ 2059 0557). At the time of the survey, there was no information available on the provenance or date of the stone and unfortunately it was stolen before detailed recording could take place

A7.4 FIELD WALLS

A7 4 1 The locations of the field walls that were recorded are depicted on the drawings that accompany the site clearance works designs. At the time of survey, the majority of the field walls, plus any other ancillary features, such as gate posts, that would be affected by the scheme were generally in a poor state of preservation, and some had sections that had been removed to create access points for site clearance works. All of the walls were of the local vernacular type, and none were considered to be of exceptional quality or design. All probably dated to the post-medieval period and some are likely to be of late twentieth-century date.

A7 4 2 A brief survey of field walls within the wider environs of the A66 was also conducted in order to ascertain the overall character of the field boundaries within the area. It was concluded that the majority of the drystone field walls were of the same type and appearance. Therefore, those field walls that would be affected by the scheme were not considered to be of special significance, and, as such, none were deemed to warrant retention *in situ* or further detailed recording. The record undertaken and reported in this document is deemed to be an appropriate and proportionate response to the importance of these features.

A7 4 3 **Gazetteer:** the following section comprises a gazetteer containing brief descriptions and photographs of the field walls and culvert headwalls that were affected by the scheme.

001	The eastern end of Gatherley Moor Quarry, from the north of the carriageway, looking south-east (Pl 64) Wall in state of disrepair, large sections missing Orientation NE-SW Height 0.5-1m Typical stone size / type 200 x 50mm – quarried limestone
002	The eastern end of Gatherley Moor Quarry, from the north of the carriageway, looking east (Pl 65) Substantial damage can be seen Orientation NE-SW Height 0.5-1m Typical stone size / type 200 x 50mm – quarried limestone
003	The eastern end of Gatherley Moor Quarry, from the north of the carriageway, looking north (Pl 66) Substantial damage is evident and the majority of the wall does not survive Orientation NE-SW Height 0.1-0.2m Typical stone size / type 200 x 50mm – quarried limestone
004	Western end of Gatherley Moor Quarry, taken from the north of the carriageway, looking south (Pl 67) Note the removal of a section of the wall at this location Orientation NE-SW Height 0.1-1m Typical stone size / type 200 x 50mm – quarried limestone
005	Western end of Gatherley Moor Quarry, taken from the north of the carriageway, looking north-west towards Carkm Moor (Pl 68) Note the removal of a substantial section of the wall at this location Orientation NE-SW Height 0.1-1.2m Typical stone size / type 200 x 50mm – quarried limestone
006	Western end of Gatherley Moor Quarry, taken from the north of the carriageway, looking north (Pl 69) Note the removal of a section of the wall at this location Orientation NE-SW Height 0.1-1.2m Typical stone size / type 200 x 50mm – quarried limestone
007	Western end of Gatherley Moor Quarry, taken from the north of the carriageway, looking north-west (Pl 70) Note the removal of a section of the wall at this location Orientation NE-SW Height 0.1-1.2m Typical stone size / type 200 x 50mm – quarried limestone
008	Field wall to the north of the A66 on the corner of Forcett Lane, looking north-west towards Carkm Moor (Pl 71) Note the similar construction style to the walls at Gatherley Moor Quarry, and the substantial damage Orientation NE-SW Height 0.1-1m Typical stone size / type 200 x 50mm – quarried limestone
009	Field wall to the south of the carriageway, taken on Forcett Lane, looking north-east (Pl 72) It appears to have been poorly rebuilt and shows signs of deterioration Note the lack of quality of its construction compared to examples at Gatherley Moor Quarry Orientation NW-SE Height 0.6-1.2m Typical stone size / type 200 x 50mm – quarried limestone

010	Field wall to the south of the carriageway taken on Forcett Lane, looking east (Pl 73) As with 009, it appears to have been poorly rebuilt and shows signs of deterioration Note the lack of quality of its construction compared to examples at Gatherley Moor Quarry Orientation NW-SE Height 0.6-1.2m Typical stone size / type 200 x 50mm – quarried limestone
011	Field wall to the south of the carriageway on the access road to Browson Bank Farm, looking north-east (Pl 74) Its constituent stones appear to be slightly larger than those at Gatherley Moor Quarry Orientation NE-SW Height c 1m Typical stone size / type 250 x 50mm – quarried limestone
012	Field wall to the north of the carriageway opposite the access road to Browson Bank Farm, looking south (Pl 75) Slightly lower than the wall at 011, but of identical form Orientation NW-SE Height c 0.5m Typical stone size / type 250 x 50mm – quarried limestone
013	Field wall at Stephen Bank, to the north of the carriageway on New Road, looking south-west (Pl 76) Similar construction to walls at 011 and 012, but in a very poor state of repair Orientation NE-SW Height 0.5-1m Typical stone size / type 300 x 50mm – quarried limestone
014	Wall on Lanehead Lane, to the north of the carriageway, looking south (Pl 77) Wall is in very degraded state Orientation NE-SW Height c 0.5m Typical stone size / type 200 x 50mm – quarried limestone
015	Detail of wall at lay-by on Stephen Bank, to the south of the existing carriageway (Pl 78) Construction is similar to that at Gatherley Moor Quarry The wall has been extensively rebuilt in places Orientation NW-SE Height c 1m Typical stone size / type 200 x 50mm – quarried limestone
016	Detail of wall at lay-by on Stephen Bank, to the south of the existing carriageway (Pl 79) Construction is similar to that at Gatherley Moor Quarry The wall has been extensively rebuilt in places, and has areas of collapse Orientation NW-SE Height c 0.5m Typical stone size / type 200 x 50mm – quarried limestone
017	Detail of wall collapse at lay-by on Stephen Bank (Pl 80) Orientation NW-SE Height c 0.5m Typical stone size / type 200 x 50mm – quarried limestone
018	Wall at Carkm Moor, to the south of the carriageway looking north-west (Pl 81), that displays evidence of stone removal and deterioration common to most of the field walls within the vicinity of the A66 Orientation NW-SE Height 0.5-0.9m Typical stone size / type 200 x 50mm – quarried limestone

019	Wall opposite Thorpe Farm, to the south of the carriageway looking south-east (Pl 82) The wall is mortared and of a different style from the drystone walls, but of a similar style to the culvert headwalls, and probably late twentieth-century in date Orientation NW-SE Height c 1m Typical stone size / type 200 x 50mm – quarried limestone
020	Possible location of Warrener trough (Pl 83, Section 4.5.5)
021	Stone headwall for culvert at the south of the carriageway to the south-east of Carkin Moor Roman fort (Pl 84) Structure is roughly 2.5m in height, and is likely to be of late twentieth-century construction

A7.5 CONCLUSIONS

A7.5.1 **Historical street furniture:** as a result of the site inspection, it was determined that three previously recorded milestones, at Rock Castle, Blackhill Farm, and at the bottom of Stephen Bank, did not appear to survive *in situ*. The Listed milestone at Thorpe Farm was seen to be set within a drystone wall, this feature was not affected by the road scheme. The possible stone trough at Warrener Lane survived *in situ*. Detailed recording of the headwalls of two culverts running beneath the A66 was undertaken (Section 4.5.5). The millstone found at Black Plantation was deserving of further analysis to determine its age and provenance, but it unfortunately disappeared before this could take place.

A7.5.2 **Field walls:** in general, the field walls affected by the scheme were found to be in a poor state of preservation, in particular where sections had already been removed to create access points. However, the walls do represent an example of vernacular drystone wall design particular to this part of the country.